Gülsüm ARIKAN

POSSIBLE INVOLVEMENT OF APOPTOSIS DURING NEURAL TRANSDIFFERENTIATION OF BONE MARROW DERIVED HUMAN MESENCHYMAL STEM CELLS BY N3 CYTOKINE COMBINATION

by

Gülsüm ARIKAN

M.S. Thesis in Biology

January 2011

January-2011

POSSIBLE INVOLVEMENT OF APOPTOSIS DURING NEURAL TRANSDIFFERENTIATION OF BONE MARROW DERIVED HUMAN MESENCHYMAL STEM CELLS BY N3 CYTOKINE COMBINATION

by

Gülsüm ARIKAN

A thesis submitted to

the Graduate Institute of Sciences and Engineering

of

Fatih University

in partial fulfillment of the requirements for the degree of

Master of Science

in

Biology

January 2011

Istanbul, Turkey

APPROVAL PAGE

I certify that this thesis satisfies all the requirements as a thesis for the degree of Master of Science.

Assist. Prof. Dr. Sevim IŞIK
Head of Department

This is to certify that I have read this thesis and that in my opinion it is fully adequate, in scope and quality, as a thesis for the degree of Master of Science.

Assist. Prof. Dr. Sevim IŞIK
Supervisor

Examining Committee Members

Assist. Prof. Dr. Lokman ALPSOY _____

Assist. Prof. Dr. Mustafa Fatih ABASIYANIK _____

Assist. Prof. Dr. İffet İrem UZONUR _____

It is approved that this thesis has been written in compliance with the formatting rules laid down by the Graduate Institute of Sciences and Engineering.

Assoc. Prof. Nurullah ARSLAN
Director

January 2011

POSSIBLE INVOLVEMENT OF APOPTOSIS DURING NEURAL TRANSDIFFERENTIATION OF BONE MARROW DERIVED HUMAN MESENCHYMAL STEM CELLS BY N3 CYTOKINE COMBINATION

Gülsüm ARIKAN

M. S. Thesis - Biology
January 2011

Supervisor: Assist. Prof. Dr. Sevim IŞIK

ABSTRACT

Apoptosis is the programmed cell death as signalled by the nuclei in normally functioning human and animal cells when age or state of cell health and condition dictates. Although apoptosis is an important tool to shape developing organs and for maintaining cellular homeostasis *in vivo,* for neural differentiation *in vitro* it is an undesirable process and it may be caused by neural inducers. Stem cells can transdifferentiate into different cell types including neuronal cells. The transdifferentiation process of stem cells might be affected by neural inducers in terms of apoptosis and cytotoxicity. In this study, we investigated the cytotoxic and apoptotic effects of neural differentiation by N3 cytokine combination (Neurobasal Medium, B-27 Supplement, dbcAMP, IBMX, hEGF, rhFGF, FGF-8, rhBDNF and L-Glutamine) on bone marrow human mesenchymal stem cells (hMSCs). According to recent studies, topoisomerase IIβ (topo IIβ) may play a role in neuronal transdifferentiation. The transdifferentiation process of stem cells appears to be different substantially from the terminal differentiation of granule neurons. Therefore, the functional significance of topo IIβ may also be different in these differentiation systems. So, topo IIβ specific small interference RNAs (siRNAs) with Lipofectamine RNAiMAX transfection reagent was also used during neural differentiation to investigate the safeness of Lipofectamine RNAiMAX transfection reagent. Then, the cytotoxicity and cell proliferation effect of Lipofectamine RNAiMAX transfection reagent on hMSCs was tested. Considering the experimental layout, hMSCs were induced by N3 cytokine combination for differentiation and siRNA transfection was performed. Next, Real Time Cell Analysis (RTCA) and apoptosis assays were carried out. After neural differentiation by N3 cytokine combination, neural differentiation efficiency of hMSCs by N3 cytokine combination was found nearly 70±10% according to changes in morphology. The axon length in siRNA transfected neural cells was shorter (55±5) than untransfected neural

cells. Next, hMSCs did not undergo apoptosis at the 2nd, 6th and14th day as determined by the Annexin and Caspase 3 assays. However, at the end of the 14th day, 10±2%, 13±1% and 15±4% necrotic cells were indicated in induction, transfection and transfection with induction group, respectively. At the 2nd and 6th day insignificant percentage of cells entered necrosis as monitored by the necrotic marker Sytox Green.

Keywords: Apoptosis, cytotoxicity, human mesenchymal stem cells, neural differentiation, siRNA transfection

KEMİK İLİĞİ KÖKENLİ İNSAN MEZENKİMAL KÖK HÜCRELERİNİN N3 SİTOKİN KOMBİNASYONU İLE NÖRAL FARKLILAŞMASI BOYUNCA APOPTOZUN OLASI İLİŞKİSİ

Gülsüm ARIKAN

Yüksek Lisans Tezi – Biyoloji
Ocak 2011

Tez Danışmanı: Yrd. Doç. Dr. Sevim IŞIK

ÖZ

Apoptoz, normal işlevli insan ve hayvan hücrelerinde, hücre sağlığının durumu veya yaşı ve durumu gerektiğinde hücre çekirdeği tarafından sinyallenen programlı bir hücre ölümüdür. Apoptoz, *in vivo*'da gelişen organların şekillenmesi ve hücresel iç dengenin düzenlenmesinde önemli bir araç olmasına rağmen *in vitro*'daki nöral farklılaşma için istenmeyen bir süreçtir ve nöral tetikleyiciler buna sebep olabilir. Kök hücreler, sinir hücrelerini de içeren farklı hücre türlerine trans-farklılaşabilir. Kök hücrelerin trans-farklılaşma süreci apoptoz ve sitotoksisite açısından nöral tetikleyiciler tarafından etkilenebilir. Bu çalışmada insan kemik iliği mezankimal kök hücreleri (iMKH) üzerinde N3 sitokin kombinasyonuyla olan nöral farklılaşmanın sitotoksik ve apoptotik etkileri çalışıldı. Yakın zamandaki çalışmalara göre, topoizomeraz IIβ (topo IIβ) nöral farklılaşmada rol alabilmektedir. Kök hücrelerin trans-farklılaşma süreci primer nöron hücrelerin farklılaşmasından daha farklıdır. Bunun için, topo IIβ'nın kök hücrelerin transdifferensiyasyon işleminde primer hücrelerin farklılaşmasındakinden farklı davranması muhtemeldir. Buna dayanarak, Lipofectamine RNAiMAX transfeksiyon maddesinin güvenilirliğine açıklık kazandırmak amacıyla nöral farklılaşmada topo IIβ'ya özel kısa interferanslar (siRNAs) ile beraber Lipofectamine RNAiMAX transfeksiyon maddesi de kullanıldı. Daha sonra, Lipofectamine RNAiMAX transfeksiyon maddesinin iMKH'ler üzerinde sitotoksisite ve apoptoz etkisi incelendi. Deneysel düzenlenme göz önüne alınarak iMKH'ler farklılaşma için N3 sitokin kombinasyonu ile indüklendi ve siRNA transfeksiyonu gerçekleştirildi. Gerçek Zamanlı Hücre Analizi (RTCA) ve apoptoz deneyleri uygulandı. N3 sitokin kombinasyonu ile nöral farklılaşmadan sonra, iMKH'lerin N3 sitokin kombinasyonu ile nöral farklılaşma verimi morfolojideki değişikliklere göre yaklaşık olarak %70±10 bulundu. siRNA ile baskılanan nöral hücrelerde akson uzunluğu siRNA uygulanmayan hücrelere göre daha kısadır (55±5). Ayrıca, iMKH'ler Annexin ve Caspase 3 testleri ile tanımlandığı gibi 2^{nci}, 6^{ncı} ve14^{üncü} günde apoptoza girmedi. Fakat 14^{üncü} günde %10±2,

%13±1 ve %15± nekrotik hücreler sırasıyla indüksiyon, transfeksiyon ve indüksiyonla beraber transfeksiyon grubunda gözlemlenmiştir. 2^{nci} ve 6^{ncı} günde önemsiz sayıda hücreler, nekrotik bir işaretleyici (marker) olan Sytox Green ile gözlendiği üzere nekroza girmişlerdir.

Anahtar Kelimeler: Apoptoz, sitotoksisite, insan mezenkimal kök hücreleri, nöral farklılaşma, siRNA transfeksiyonu

To the loved One and to all of his unique names

ACKNOWLEDGEMENT

I want to express my appreciation to my thesis supervisor Assist. Prof. Dr. Sevim IŞIK for her patience, great contribution to my academic progress and giving me an opportunity to understand what scientific life is. I also would like to thank to all of my instructors in Fatih University.

I would like to thank my lab-mates Nebiyyeh KAMACI, Nihal KARAKAŞ, Tuğba SAĞIR, Tuba EMNACAR, Merve ZAİM and Aysel KARAGÖZ also to my colleagues for their support and friendship during and after our master education.

I am very fortunate to have the opportunity of being friends with Ayşe DEMİR and Zehra DURMUŞ who have accompanied me in my hard and good times.

This work was supported by TÜBİTAK Project No. 106S279 and Fatih University Project No. P50030706 (391).

TABLE OF CONTENTS

LIST OF TABLES

TABLE

LIST OF FIGURES

FIGURE

LIST OF SYMBOLS AND ABBREVIATIONS

SYMBOL	ABBREVIATION
MSC	Mesenchymal stem cell
hMSC	Human mesenchymal stem cell
BM	Bone marrow
DMEM	Dulbecco's modified Eagle's medium
FBS	Fetal Bovine Serum
CO_2	Carbon dioxide
FACS	Fluorescence activated cell sorting
IBMX	3-Isobutyl-1-methylxanthine
RT-PCR	Reverse transcriptase polymerase chain reaction
VCAM-1	Vascular cell adhesion molecule
F-CFU	Fibroblast Colony Forming Units
GM-SCF	Granulocyte-Macrophage Colony-Stimulating Factor
SCF	Stem cell factor
HGF	Hepatocyte growth factor
GVHD	Graft versus host disease
HSCs	Haematopoietic stem cells
dsRNA	Double stranded RNA
LDH	Lactate dehydrogenase
EC	Electron coupling reagent
RS	Mitochondrial succinate-tetrazolium-reductase system
RTCA	Real Time Cell Analysis
RT-CES	Real-time cell electronic sensing
TNF	Tumor necrosis factor
DISC	Death-inducing signaling complex

FADD	Fas-associated death domain
TRADD	TNF receptor-associated death domain
FasL	Fatty acid synthetase ligand
FasR	Fatty acid synthetase receptor
RIP	Receptor-interacting protein
MPT	Mitochondrial permeability transition
Smac/DIABLO	Second mitochondrial activator of caspases/direct IAP binding protein with low PI
HtrA2/Omi	High-temperature requirement
Apaf-1	Apoptotic protease activating factor
CTLs	Cytotoxic T lymphocytes
EM	Electron microscopy
LM	Light microscopy
FC	Flow cytometry
TUNEL	Terminal dUTP Nick End-Labeling
Bcl-2	B-cell lymphoma protein 2
IAP	Inhibitor of Apoptosis Proteins
BH	Bcl-2 homology
TM	Transmembrane
MOMP	Mitochondrial outer membrane permeabilization
NIM	Neuronal induction medium
bFGF	Basic fibroblast growth factor
EGF	Epidermal growth factor
dbcAMP	dibutyryl cyclic AMP
DMSO	Dimethylsulfoxide
RA	Retinoic acid
BDNF	Brain-derived neurotrophic factor
BME, β-ME	β-mercaptoethanol
BHA	Butylated hydroxyanisole
Topo II	Topoisomerase II
Topo IIα	Topoisomerase IIα
Topo IIβ	Topoisomerase IIβ
RNAi	RNA interference
siRNA	Small interference RNA

RISC	RNA-Induced Silencing Complex
mRNA	Messenger RNA
cDNA	Complementary DNA
CAM	Camptothecin

CHAPTER 1

INTRODUCTION

1.1 MESENCHYMAL STEM CELLS

1.1.1 Definition and Sources of MSCs

Mesenchymal stem cells (MSCs) are multipotent stem cells which possess an extensive proliferative potential and ability to differentiate into various cell types, including: osteocytes, adipocytes, chondrocytes, myocytes, cardiomyocytes and neurons [1].

The main source of MSCs is the bone marrow. These cells constitute, however, only a small percentage of the total number of bone marrow populating cells. Pittenger *et al.* showed that only 0.01% to 0.001% of mononuclear cells isolated on density gradient (ficoll/percoll) give rise to plastic adherent fibroblast-like colonies. Apart from the bone marrow, MSCs are also located in other tissues of the human body. There is an increasing number of reports describing their presence in adipose tissue [2], umbilical cord blood, chorionic villi of the placenta [3], amniotic fluid [4], peripheral blood, fetal liver, lung, and even in exfoliated deciduous teeth [1].

The minimal requirement for a population of cells to qualify as MSCs, as suggested by the International Society for Cytotherapy, is to meet the three criteria, including

(i) the plastic adherence of the isolated cells in culture,

(ii) the expression of CD105, CD73, and CD90 in greater than 95% of the culture, and their lack of expression of markers including CD34, CD45, CD14 or CD11b, CD79a or CD19 and HLA-DR in greater than 95% of the culture,

(iii) the differentiation of the MSCs into bone, fat and cartilage [5].

1.1.2 Biology of MSCs

MSCs form a heterogeneous population of cells, regarding their morphology, physiology and expression of surface antigens. MCSs express a large number of adhesion molecules, extracellular matrix proteins, cytokines and growth factor receptors, associated with their function and cell interactions within the bone marrow stroma [6]. They also express a wide variety of antigens characteristic for other cell types. The population of MSCs isolated from bone marrow express: CD44, CD105 (SH2; endoglin), CD106 (vascular cell adhesion molecule; VCAM-1), CD166, CD29, CD73 (SH3 and SH4), CD90 (Thy-1), CD117, STRO-1 and Sca-1 [7]. Parallelly, MSCs do not possess markers typical for hematopoietic and endothelial cell lineages: CD11b, CD14, CD31, CD33, CD34, CD133 and CD45. The absence of CD14, CD34 and CD45 antigens on their surface create the basis to distinguish them from the hematopoietic precursors [8].

1.1.3 Historical Overview of MSCs

In the development of mesenchymal stem cell concept, Friedenstein and his colleagues played a key role. In their studies during 1960s and 70s, they described clonal and plastic adherent stromal cells from bone marrow. In additon to that, they demonstrated that these cells formed fibroblast colony forming units (F-CFU) and also had the capacity to differentiate towards osteoblasts, chondroblasts and adipocytes under defined in vitro culture conditions [9].

1.1.4 Function of MSCs

MSCs play a crucial role in bone marrow microenvironment. The main function of them is to build a tissue framework, which provides a mechanical support for hematopoietic cell system. They secrete a number of extracellular matrix proteins, including fibronectin, laminin, collagen and proteoglycans [10]. Moreover, hematopoietic and non-hematopoietic growth factors like chemokines and cytokines are produced by MSCs, thereby MSCs function in the regulation of hemopoiesis. MSCs secrete: IL-1a, IL-1b, IL-6, IL- 7, IL-8, IL-11, IL-14, IL-15, macrophage colony-stimulating factor, granulocyte-macrophage colony-stimulating factor (GM-SCF), leukemia inhibitory factor, stem cell factor (SCF), fetal liver tyrosine kinase-3, thrombopoietin and hepatocyte growth factor (HGF) [11]. Some of these proteins are produced by inactive cells, whereas the others after stimulation. The involvement of MSCs in hematopoiesis is additionally combined by their presence in fetal liver and bone marrow for the onset of ultimate hemopoiesis at those sites.

Among other well known biological activities of MSCs, it is worth to point out their immunomodulatory functions [1]. These cells are able to inhibit responses of alloreactive T lymphocytes. MSC-mediated immunosuppression involves preparatory activation of the MSCs by immune cells through the secretion of the proinflammatory cytokine IFNγ, alone or together with TNFα, IL-1α or IL-1β [10]. This activation step has also been shown *in vivo* in a model of graft versus host disease (GVHD). Thus, the immunosuppressive effect of MSCs on T lymphocytes would function to stop self responses in both physiological and pathological conditions.

1.1.5 Differentiation Potential of MSCs

The adult bone marrow contains two prototypical stem cell populations: haematopoietic stem cells (HSCs) and mesenchymal stem cells also called bone marrow stromal cells. Both haematopoietic stem cells (HSCs) and MSCs are of mesoderm origin. Whereas HSCs give rise to the various blood cells, MSCs can differentiate into mesenchymal derivatives, including osteocytes, chondrocytes, adipocytes, and myocytes. In addition, MSCs play a role in providing the stromal support system for HSCs in the bone marrow [12]. MSCs have also been reported to differentiate into

myocytes and cardiomyocytes and even into cells of non-mesodermal origin, including hepatocytes, insulin-producing cells, and neurons [5].

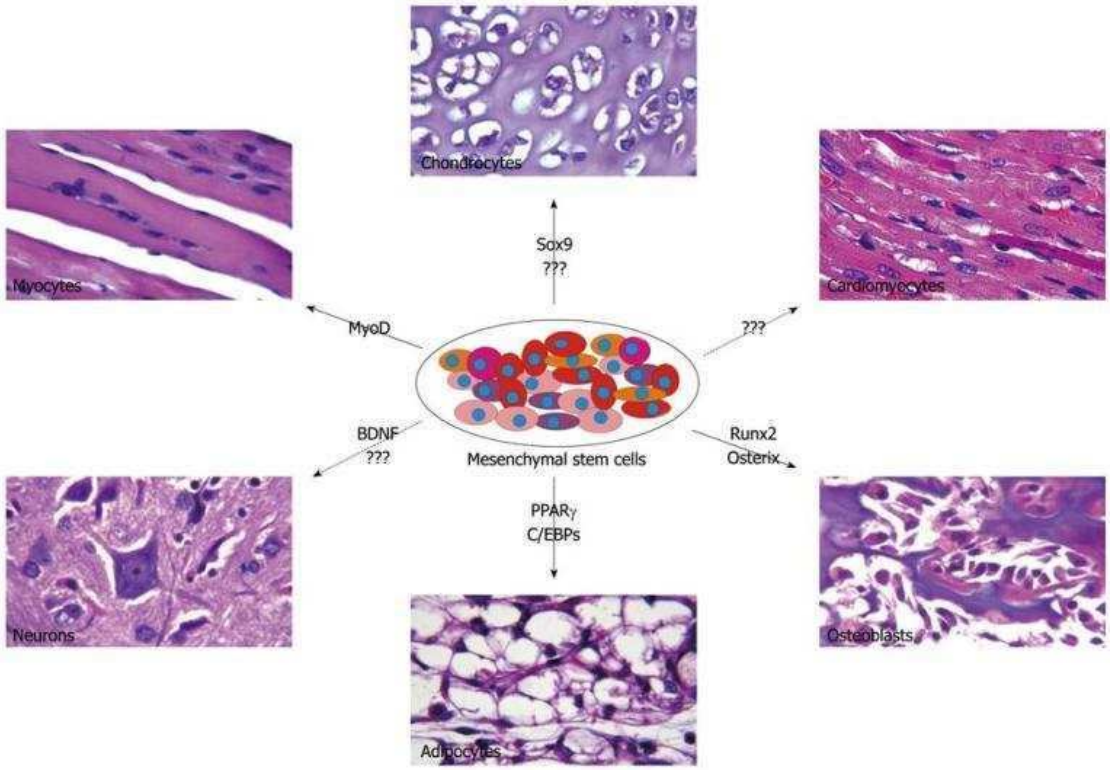

Figure 1.1 Pluripotent capacity of MSC to differentiate into mesodermal and nonmesodermal cell lineages, including osteocytes, adipocytes, chondrocytes, myocytes, cardiomyocytes, and neurons. The lineage-specific differentiation is a multi-stage and well-coordinated process controlled by key regulators. Runx2 and Osterix are important master regulators for osteogenic differentiation while peroxisome proliferator-activated receptor γ and CCAAT/enhancer binding protein β are important factors promoting adipogenesis. SRY-box 9 is the main regulator of chondrogenic regulation while MyoD plays a key role in myogenic differentiation [13].

1.1.6 Potential Clinical Applications of MSC

Since MSCs are multipotent and their numbers can be expanded in culture, there has been much interest in their clinical potential for tissue repair and gene therapy. A number of studies have now also demonstrated the migration and multi-organ engraftment potential of MSCs in animal models and in various human organ transplantations. In addition, immunomodulatory properties of MSC and their supportive functions for haematopoietic stem cells have also opened up possibilities for

interesting new avenues for their use in the treatment of autoimmune diseases and graft rejection, respectively [9].

Stem cell therapy involves the transplantation of autologous or allogeneic stem cells into patients, either through local delivery or systemic infusion. There is a precedent in hematopoietic stem cell transplantation, which has been used for some years in the treatment of leukemia and other cancers. Some striking examples of the therapeutic use of marrow-derived MSCs have been reported recently. These address a broad spectrum of indications, including cardiovascular repair, treatment of lung fibrosis, spinal cord injury and bone and cartilage repair. For instance, stem cells with the ability to differentiate into neurons, astrocytes and oligodendrocytes have been isolated from rat spinal cord and implantation of neural stem cells in an adult rat model of spinal cord injury resulted in long-term functional improvement [14].

1.2 DNA TOPOISOMERASES AND THEIR ROLE IN NEURAL DIFFERENTIATION

The physical integrity and organization of chromosomal DNA are maintained throughout a cell's life. Unfortunately, a number of essential cellular processes can have adverse effects on DNA superstructure. For instance, at DNA replication, recombination, chromatin remodeling, and transcription superhelical tension occurs in the adjacent double helical region. DNA topoisomerases solve the topological problems associated with DNA replication, transcription, recombination, and chromatin remodeling by introducing temporary single- or double-strand breaks in the DNA [15].

Topoisomerases are classified into two types as type I and II topoisomerases and separated by the number of strands cut in one round of action. Moreover, these enzymes are structurally and mechanistically different. Type I enzymes introduce a single stranded break in DNA while type II enzymes are dimeric enzymes that can introduce a break in two strands at the same time. Different from type I topoisomerases, type II topoisomerases use ATP during changing DNA topology.

Type II topoisomerases modulate the topology of DNA and relieve supercoil stress. It provides a transient cleavage of DNA strands and allows a second double-stranded DNA segment pass through the gate. Different from other topoisomerases this transport is an ATP coupled process at type II topoisomerases. This ATP coupling is

necessary for the enzyme to return its initial configuration. After the DNA transport the double-strand break is relegated [16].

There are two subclasses of type II topoisomerases, type IIA and type IIB. Type IIA topoisomerases are the enzmes DNA gyrase, eukaryotic topoisomerase II and bacterial topoisomerase IV. Type IIB topoisomerases are distinct from type IIA and found in archea and higher plants.

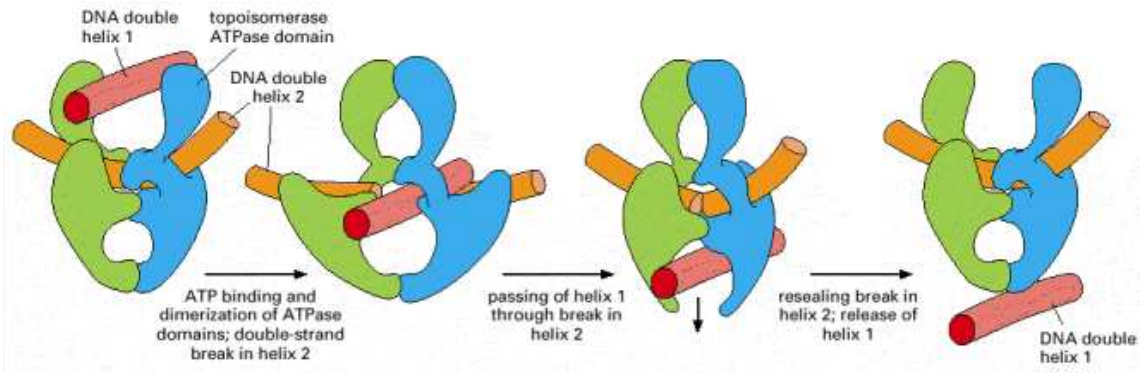

Figure 1.2 Action mechanism of DNA topoisomerase II [17].

DNA topoisomerase II enzymes have three domains; ATPase domain, DNA cleavage domain, and C-terminal domain. In mammalian cells two isoforms of topoisomerase II have been identified; 170- kDa topoisomerase IIα (topo IIα) and the 180-kDa topoisomerase IIβ (topo IIβ). These isoforms are encoded by separate genes but they are similar in primary structure (72%) and they have similar catalytic properties *in vitro*. However they are regulated very differently.

Topo IIα expression is cell cycle-dependent since its level rises during S phase and it reaches its peak at the G2/M phase of the cell cycle. Moreover, it is preferentially expressed in proliferating cells while topo IIβ expression is not dependent on cell cycle and expressed both in proliferating and quiescent cells. Furthermore, topo IIα plays an important role in cell cycle events such as DNA replication and chromosome condensation/segregation. On the other hand, the abundance of topo IIβ in terminally differentiated cells suggests that it may play a role in DNA metabolism other than DNA replication and chromosome condensation/segregation.

1.2.1 Role of Topoisomerase IIβ in Neural Differentiation

Topoisomerase IIβ is found to be highly expressed in post-mitotic cells that are committed to differentiate into neural cells. Tsutsui et al. showed that topo IIβ is highly expressed in differentiating cerebellar neurons [18]. And whole body topIIβ knockout mice have shown prenatal death. It was found that topo IIβ play a role in activation or repression of developmentally regulated genes at late stages of neuronal differentiation.

Yang et al found that motor axons in topoIIβ $^{-/-}$ embryos failed to contact skeletal muscles and sensory axons were not able to enter spinal cord. Presynaptic nerve terminals and axons were found to be absent in topoIIβ $^{-/-}$ embryos [19]. Nur-E-Kamal et al. reported that topoIIβ plays critical role in neurite outgrowth and growth cone formation during neural differentiation and may affect neurite outgrowth through its regulation of the expression of certain neuronal genes. Cortical neurons isolated from topoIIβ knockout mice embryos also exhibited shorter neurons indicating the role of topoIIβ in neurite outgrowth [20].

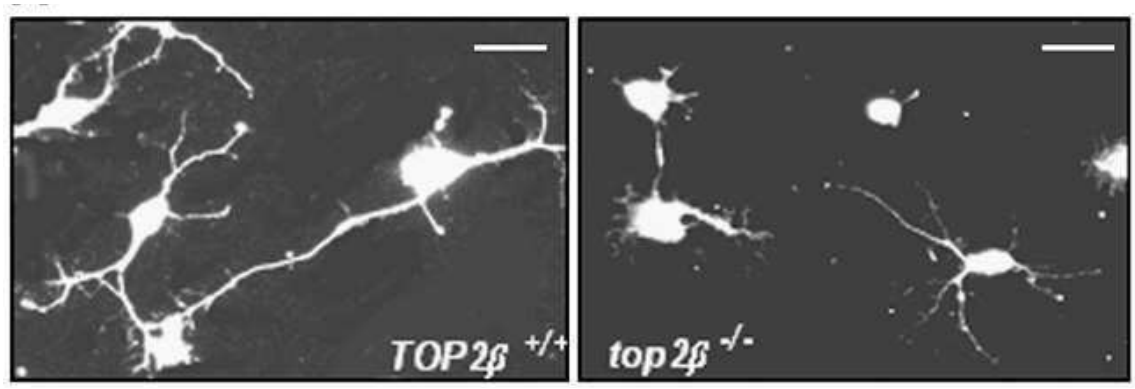

Figure 1.3 Neurons from topoIIβ$^{-/-}$ mouse brains cannot extend neurites in culture [20].

1.3. RNA INTERFERENCE

RNA interference (RNAi) is one of the most exciting discoveries of the past decade in the field of genomics. It is a phenomenon in which double stranded RNA (dsRNA) is the initiating factor in post-transcriptional gene silencing. It is a process in which the introduction of a double stranded RNA (dsRNA) into cells causes the specific degradation of mRNA containing the same sequence.

1.3.1 The Mechanism of RNA Interference

RNAi is a two-step mechanism. Firstly, long dsRNAs are cleaved by an enzyme known as DICER in 21–23 nucleotides fragments (siRNAs). Secondly, siRNAs are recruited to RNA Induced Silencing Complex (RISC) and in turn mediates the cleavage of the target mRNA.

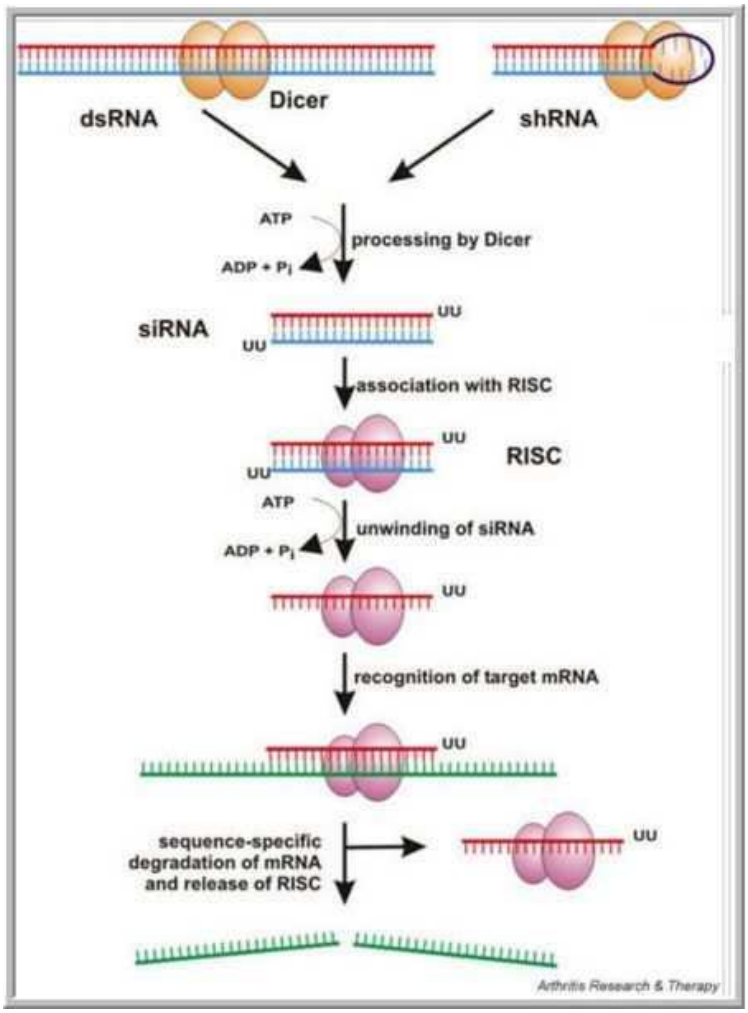

Figure 1.4 The mechanism of RNA interference [21].

1.4. CYTOTOXICITY AND CELL PROLIFERATION

1.4.1 Cytotoxicity Assay

Cell death is typically measured by the quantification of plasma membrane damage. Cytotoxicity assay is based on the measurement of cytoplasmic enzyme activity released by damaged cells. The amount of enzyme activity detected in the culture supernatant correlates to the proportion of lysed cells. Lactate dehydrogenase

(LDH) is a stable cytoplasmic enzyme present in all cells. It is quickly released into the cell culture supernatant upon damage of the plasma membrane. The LDH activity is identified in an enzymatic test: In the first step NAD+ is reduced to NADH/H+ by the LDH-catalyzed conversion of lactate to pyruvate. In the second step the catalyst (diaphorase) transfers H/H+ from NADH/H+ to the tetrazolium salt INT which is reduced to formazan.

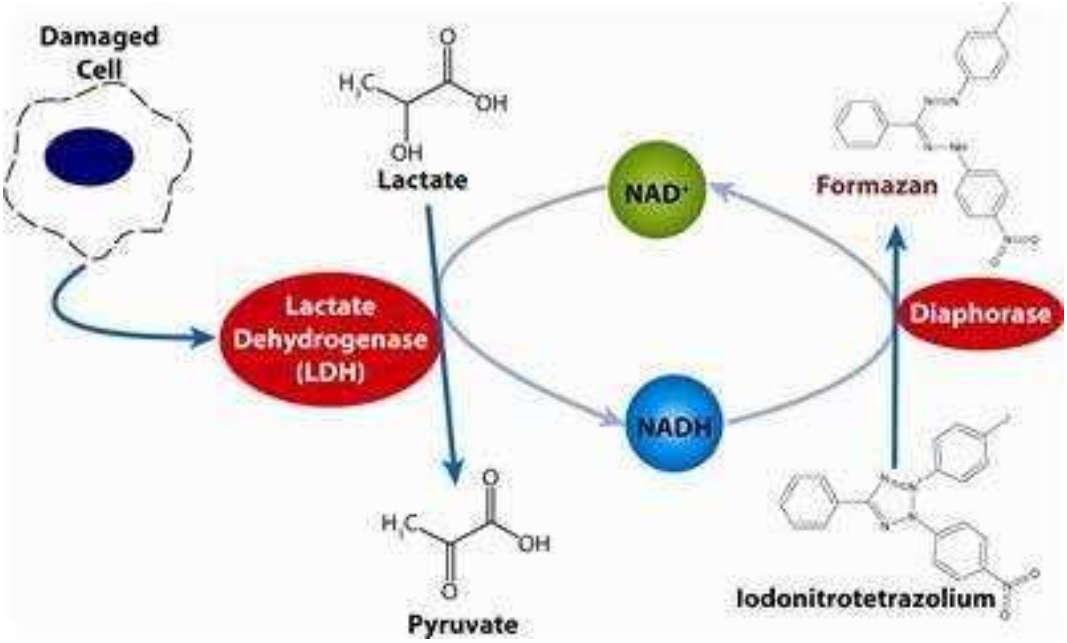

Figure 1.5 The mechanism of LDH assay. In the first step, released lactate dehydrogenase (LDH) reduces NAD+ to NADH+ H+ by oxidation of lactate to pyruvate. In the second enzymatic reaction 2 H are transferred from NADH+ H+ to the yellow tetrazolium salt INT (2-[4-iodophenyl]-3-[4-nitrophenyl]-5-phenyltetrazolium chloride) by a catalyst [22].

An increase in the amount of dead or plasma membrane-damaged cells results in an increase of the LDH enzyme activity in the culture supernatant. This increase in the amount of enzyme activity in the supernatant directly correlates to the amount of formazan formed during a limited time period. Therefore, the amount of color formed in the assay is proportional to the number of lysed cells.

1.4.2 Cell Proliferation Assay

Proliferation assays have become available for analyzing the number of viable cells by the cleavage of tetrazolium salts added to the culture medium. The tetrazolium salts are cleaved to formazan by cellular enzymes. An expansion in the number of viable cells results in an increase in the overall activity of mitochondrial dehydrogenases in the sample. This rise in enzyme activity leads to an increase in the amount of formazan dye formed, which directly correlates to the number of metabolically active cells in the culture.

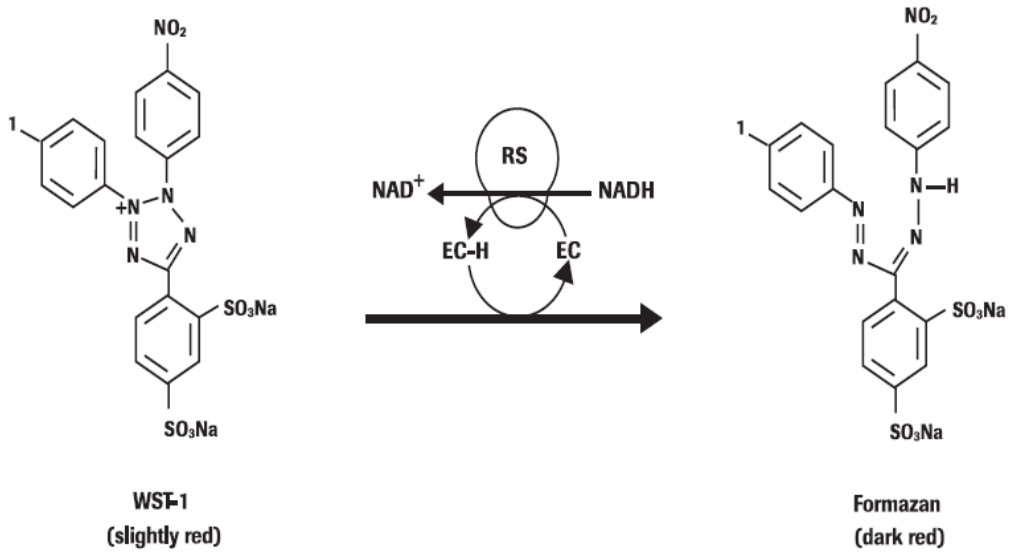

Figure 1.6 Cleavage of the tetrazolium salt WST-1 (4-[3-(4-Iodophenyl)-2-(4-nitrophenyl)- 2H-5-tetrazolio]-1,3-benzene disulfonate) to formazan. (EC = electron coupling reagent RS = mitochondrial succinate-tetrazolium-reductase system) [23].

1.4.3 Real Time Cell Analysis (RTCA)

Real-time cell electronic sensing (RT-CES; now known as xCELLigence RT-CA) system (Figure 1.7) uses microelectronic plates (E-Plates) integrated with gold microelectrode arrays on glass substrate in the bottom of the wells to measure cellular status in real time [24]. In the presence of media, application of low AC voltage (10 mV) produces a small electric field between the electrodes that can be impeded by the presence of adherent mammalian cells leading to large changes in measured impedance. The extent of impedance change is proportional to the number of cells inside the well and the inherent morphological and adhesive characteristics of the cells.

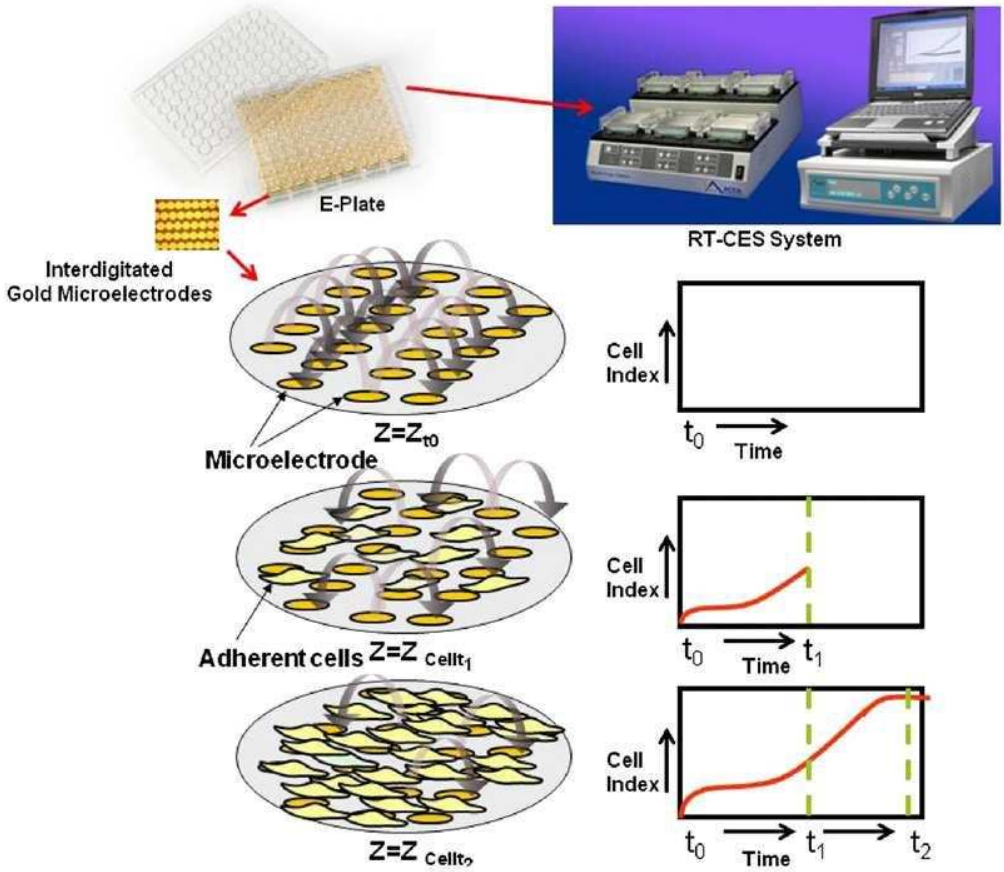

Figure 1.7 Real-Time Monitoring of Adherent Cells by the RT-CES System [25].

The RT-CES system is composed of a plate station accommodating up to six 96 well E-Plates, an electronic analyzer, and a computer that runs the software for automatic and real-time data acquisition and display. The E-Plates are integrated with interdigitated gold microelectrodes. A schematic representation of microelectrodes and the principle of using cell electrode impedance to noninvasively measure adherent cells are shown. In the absence of cells, the baseline impedance (Z_0) at time zero (t_0) represents the impedance of the gold microelectrodes. Addition of cells to the sensor microelectrodes leads to changes in impedance signal at time t_1 (Z_{cellt1}) that is directly proportional to the number of cells seeded on the sensors and is displayed as the cell index. The cell index value changes with time (Z_{cellt2}) and reflects the morphology, adhesion, and number of cells inside the well [25].

1.5 CLASSIFICATION OF CELL DEATH

Cell death is known to be perpetrated through a variety of mechanisms. According to Galluzzi et al., cell death can be classified into three different types, based upon morphological characteristics: apoptosis, necrosis (oncosis) and autophagy. The morphological changes accompanying apoptosis will be described in detail below. Whereas apoptosis is manifested by volume reduction of the nucleus and cytoplasm (cell shrinkage), necrosis (the mode of cell death with which apoptosis is most often confused) is evinced by cytoplasmic swelling, rupture of the plasma membrane, swelling of cytoplasmic organelles (particularly mitochondria), and some condensation of nuclear chromatin [26]. Autophagy is distinguished by the accumulation of cytoplasmic vacuoles and membranes.

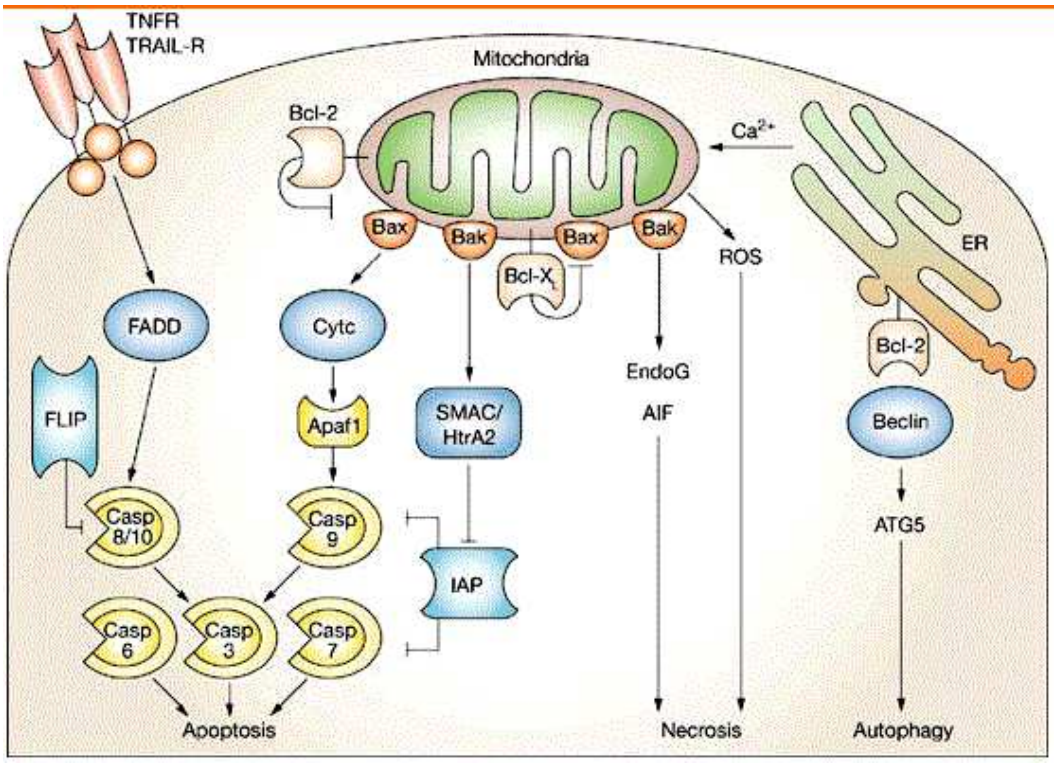

Figure 1.8 Schematic diagram representing the pathways of apoptosis, necrosis and autophagy [27].

1.5.1 Apoptosis

Apoptosis is programmed cell death, which involves the genetically determined elimination of cells. Apoptosis occurs normally during development and aging and as a homeostatic mechanism to maintain cell populations in tissues. For instance, during normal morphogenesis in order to discard unneeded cells apoptosis plays a key role resulting in well-formed, functional tissues. Apoptosis also occurs as a defense mechanism such as in immune reactions or when cells are damaged by disease or noxious agents [28].

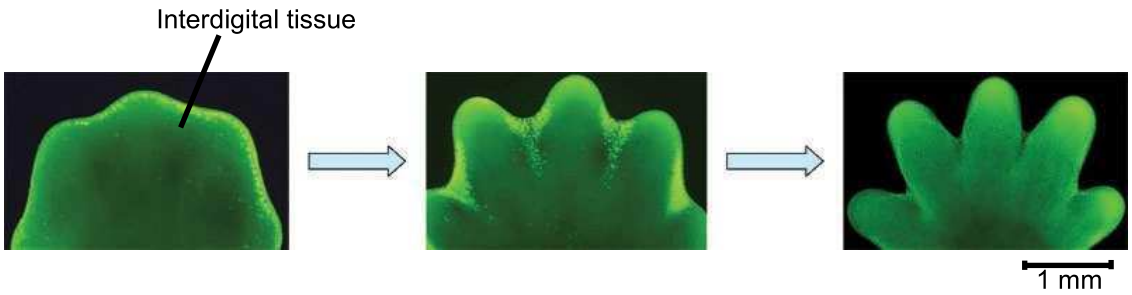

Figure 1.9 Effect of apoptosis during paw development in the mouse [29].

Apoptosis has characteristic morphologic and biochemical signs, the most important of them being accumulation of phosphatidylserine in the outer monolayer of the cytoplasmic membrane, condensation of chromatin, fragmentation of DNA, disintegration of cells into apoptotic vesicles [30].

Apoptotic cell death was first described by Kerr *et al.* in 1972 and was distinguished from necrotic cell death based on morphological criteria, such as condensation of chromatin at the nuclear periphery, disassembly of nuclear scaffold proteins, and the formation of apoptotic bodies [31]. The first biochemical evidence of apoptosis was reported by Skalka *et al.* (1976), when the DNA of lymphocytes irradiated *in vivo* was shown to be degraded into oligo nucleosomal length fragments. This event was subsequently linked to endonuclease activity [32] and has since become a prominent and routinely used biochemical marker of apoptosis [33].

1.5.1.1 Features of Apoptosis

Apoptotic cells are examined in a wide variety of tissues, involving during development and neoplastic transformation. Although scientists could detect apoptotic cells in many cases by light microscopy, it was their observations by transmission electron microscopy that introduced the characteristic ultrastructural features known as the hallmark of apoptosis. These features include (1) cytoplasmic and nuclear condensation (pyknosis); (2) nuclear fragmentation (karyorrhexis); (3) normal morphological appearance of cytoplasmic organelles; and (4) an intact plasma membrane. Commonly, the pyknotic nucleus appears in a crescent shape, a feature most indicative of an apoptotic cell (Figure 1.10). After nuclear fragmentation, the cell disaggregates into membrane-bound apoptotic bodies, which are engulfed through phagocytosis by neighboring epithelial cells or macrophages [34].

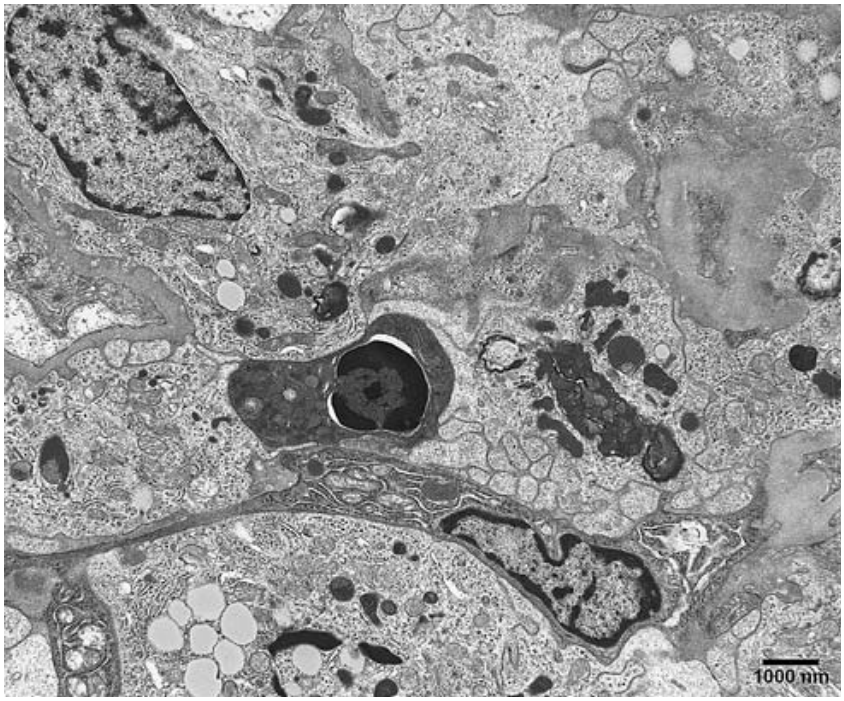

Figure 1.10 Transmission electron microscopic image of an apoptotic cell in a human kidney biopsy. Note the pyknotic, shrunken nucleus and the very condensed cytoplasm [34].

1.5.1.2 Fundamental Mechanisms of Apoptosis

The mechanisms of apoptosis are highly complicated and developed, including an energy-dependent cascade of molecular events. Until now, recent studies report that there are two main apoptotic pathways: the extrinsic or death receptor pathway and the intrinsic or mitochondrial pathway. Nevertheless, there is now evidence that the two pathways are related and the molecules of one pathway can influence the other.

There is an extra pathway that includes T-cell mediated cytotoxicity and perforin-granzyme-dependent killing of the cell. The perforin/granzyme pathway can cause apoptosis via either granzyme B or granzyme A. The extrinsic, intrinsic, and granzyme B pathways converge on the same terminal, or execution pathway. This pathway is begun by the cleavage of caspase-3 and leads in DNA fragmentation, degradation of cytoskeletal and nuclear proteins, cross-linking of proteins, formation of apoptotic bodies, expression of ligands for phagocytic cell receptors and eventually uptake by phagocytic cells [28] .

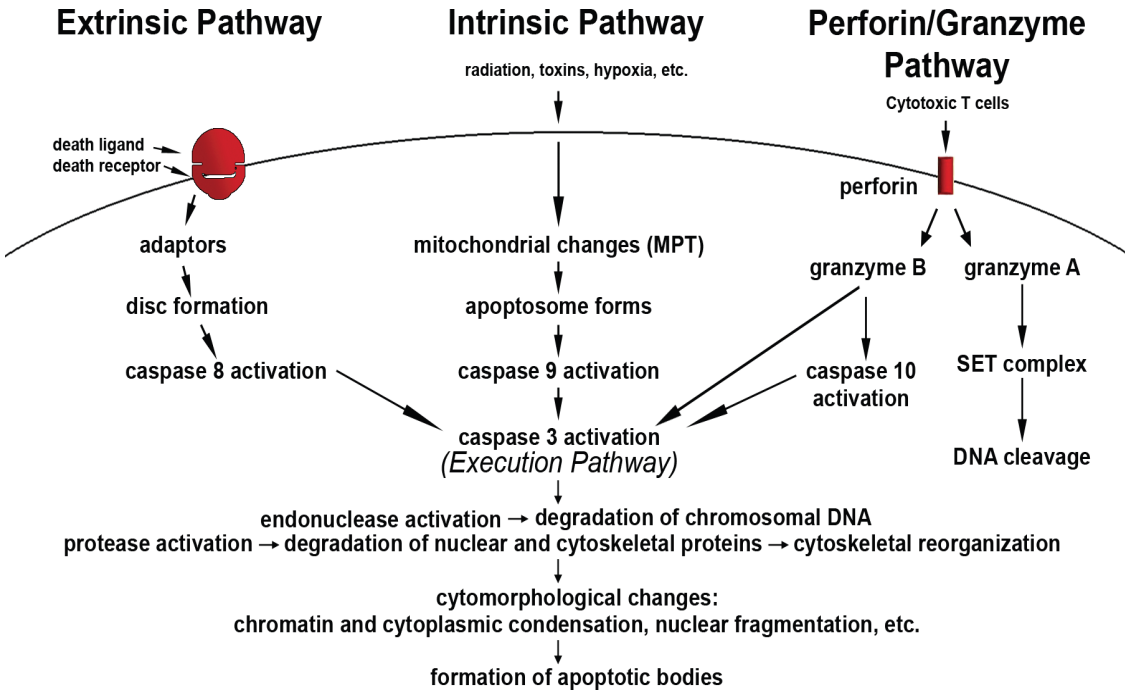

Figure 1.11 Schematic representation of apoptotic events [28].

1.5.1.2.1 Extrinsic Pathway

The extrinsic signaling pathways that cause apoptosis include transmembrane receptor-mediated interactions. The current interactions involve death receptors that are members of the tumor necrosis factor (TNF) receptor gene superfamily [35]. Members of the TNF receptor family have similar cyteine-rich extracellular domains in common and have a cytoplasmic domain of about 80 amino acids named the “death domain” [36]. The death domain has a crucial role in transmitting the death signal from the cell surface to the intracellular signaling pathways. Until now, the best-characterized ligands and corresponding death receptors involve FasL/FasR, TNF-α/TNFR1, Apo3L/DR3, Apo2L/DR4 and Apo2L/DR5.

The succession of events that determine the extrinsic phase of apoptosis are distinguished by the FasL/FasR and TNF-α/TNFR1 models. In these models, there is assembling of receptors and binding with the homologous trimeric ligand. Upon ligand binding, cytplasmic adapter proteins are engaged which exhibit corresponding death domains that bind with the receptors. The binding of Fas ligand to Fas receptor leads to the binding of the adapter protein FADD and the binding of TNF ligand to TNF receptor results in the binding of the adapter protein TRADD with recruitment of FADD and RIP. Next, FADD connects with procaspase-8 by dimerization of the death effector domain. At this juncture, a death-inducing signaling complex (DISC) is formed, leading to the autocatalytic activation of procaspase-8. As caspase-8 is activated, the execution phase of apoptosis is initiated [28].

1.5.1.2.2 Intrinsic Pathway

In the intrinsic pathway, a wide range of stimuli produced by non-receptors stimulate intracellular pathways causing apoptosis either by initiating events in the cell or by targeting the mitochondrial initiated signals. These stimuli produce positive or negative intracellular signals: Positive signals are stimulated by factors such as radiation, free radicals, viral infections, toxins hypothermia, etc. Hormones, certain growth factors, and cytokines that can lead to failure of suppression of death programs are absent in the negative signals, hence apoptosis is triggered.

These stimuli that initiate the intrinsic pathway cause alterations in the inner mitochondrial membrane that lead to such events: the mitochondrial permeability transition (MPT) pore is opened followed by the loss of the mitochondrial transmembrane potential and lastly two main groups of normally sequestered pro-apoptotic proteins from the intermembrane space into the cytosol are released. AIF, endonuclease G and CAD belong to the second group of pro-apoptotic proteins while the cytochrome *c*, Smac/DIABLO, and the serine protease HtrA2/Omi make up the first group which activate the caspase-dependent mitochondrial pathway. Both cytochrome *c* and procaspase-9 bind and activate Apaf-1, building an "apoptosome" and hence activating caspase-9 [28].

1.5.1.2.3 Perforin/granzyme Pathway

Although cytotoxic T lymphocytes (CTLs) use the extrinsic pathway and the FasL/FasR interaction is the primary method of CTL-induced apoptosis, Perforin/granzyme pathway is another major apoptosis mechanism also used by CTLs to kill tumor cells and virus-infected cells via a pathway. In the perforin/granzyme pathway, the transmembrane pore-forming molecule perforin is released together with degranulation of serine proteases, granzymes through the pore and into the target cell. The serine proteases granzyme A and granzyme B are the main effector components within the granules [37].

Granzyme B induces pro-caspase-10 activation by the cleavage of proteins at aspartate residues and directly activates caspase-3. In the case of caspase-3 induction, the upstream signaling pathways are bypassed and the execution phase of apoptosis is directly activated.

Granzyme A is another abundant granzyme that is important in cytotoxic T cell-induced apoptosis, activating caspase independent pathways. Granzyme A protease cleaves the nucleosome assembly protein SET resulting in apoptotic DNA degradation. The SET complex composed of proteins SET, Ape1, pp32, and HMG2 and these protect chromatin structure and DNA repair. Therefore, the cleavage of this complex by granzyme A leads to its inactivation and thus may contribute to apoptosis by blocking the DNA maintenance and the integrity of the chromatin structure [38].

1.5.1.3 Apoptosis Detection Methods

The original techniques to detect apoptosis involved the early definition of apoptosis based on morphology. Through the last decade, techniques have been expanded to biochemistry, molecular biology and immunology because of our increasing knowledge about the molecular mechanisms of apoptosis. Regardless of our extending insight in the initiation phase of apoptosis, most of these techniques are based on the events happening during the execution phase [39].

1.5.1.3.1 Morphological Changes

Electron Microscopy

The differences in the specific morphological changes that cells underwent in apoptosis in comparison to necrosis were first observed by electron microscopy (EM). As such it is the gold-standard test to distinguish between the two. The specific morphological changes in early and late apoptosis that can be detected with EM are depicted in Figure 1.10.

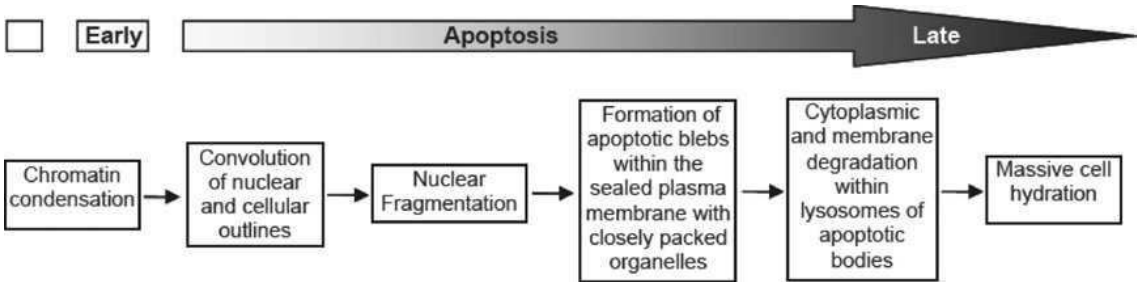

Figure 1.12 Morphological changes occurring during early and late apoptosis [40].

Light Microscopy and Fluorescence Microscopy

The earliest technique to detect apoptosis is to study the morphology of the cell by LM. Membrane blebbing, nuclear pyknosis and fragmentation can thus be visualized on haematoxylin and eosin stained histological sections. A disadvantage of LM, however, is its low sensitivity especially, since apoptotic cells are rapidly removed from the tissues by phagocytosis, which can be completed within 30–60 min following the onset of apoptosis.

The acuity of light microscopy can also be enhanced by the use of fluorescence. Nuclear fluorescent dyes such as Hoechst 33258 can be used to visualize nuclear changes.

Annexin-V

The biochemical and morphological changes caused by apoptosis affect all aspects of the cell from the plasma membrane to the nucleus. The plasma membrane is composed of a variety of phospholipids including both aminophospholipids (phosphatidylserine, PS, and phosphatidylethanolamine) and choline phospholipids (phosphatidylcholine, sphingomyelin). In the normal cellular state, the cell maintains an asymmetry between the phospholipid content of the inner and outer leaflet of the plasma membrane by actively translocating PS from the outer to the inner leaflet. In apoptosis, this asymmetry is lost as PS equilibrates between the inner and outer leaflets, a process that is facilitated by a Ca^{2+}-dependent flip-flop. The presence of PS on the outer cell surface can be detected using the PS-binding protein, annexin-V, and is a sign for neighboring cells and macrophages to remove the apoptotic cell.

Another prominent apoptotic change affecting the structure of the plasma membrane is the formation of blebs, or small, membrane-enclosed pieces of cytoplasm and condensed nuclear material. One of the final signs to appear during apoptosis is the inability of the plasma membrane to exclude dyes (e.g., trypan blue, ethidium bromide, and propidium iodide) which provides a convient way to monitor cell death [41].

1.5.1.3.2 DNA Fragmentation

TUNEL Assay

TUNEL assay is among the most widely used methods for apoptotic detection based on the fact that during apoptosis, a cation-dependent endonuclase cleaves genomic DNA between nucleosomes. Thus, DNA fragmentation during apoptosis can be detected using a fluorescent TUNEL assay.

DNA Laddering

The internucleosomal fragmentation produced by endonucleases at expected intervals of 180 base pairs to 200 base pairs is part of the biochemical hallmark of apoptosis. Standard DNA extraction techniques are used to obtain the nucleic acids from either cells or homogenized tissue. DNA is then electrophoresed in an agarose gel that demonstrates the characteristic DNA laddering pattern.

DNA Content by FC

The DNA content reflects grossly its phase in the cell cycle (G0/G1, S/G2 and M). Apoptotic cells show a decreased DNA content below the G0/G1 level. This can be measured by FC and DNA probes like propidium iodide. This technique also discriminates between apoptosis and necrosis.

1.5.1.3.3 Cytoplasmic Changes

Caspase Activity

Caspases form a family of cysteine proteases that cleave target proteins at an aspartate residue in a recognition sequence. They reside in the cytoplasm and in organelles as inactive precursors and are initiated by cleavage after specific aspartate residues. Presently various fluorogenic and chromogenic substrates are available for different active caspases.

Caspase activity can also be measured by immuno-histochemical techniques using antibodies against neoepitopes, which arise from their proteolytic activation. Caspase activity can also be detected immunologically by using antibodies, which recognize only the cleaved substrates of caspases. Recently, antibodies were described which recognize caspase cleaved cytokeratin 18, actin and PARP. Moreover, caspase activity can be detected by RT-PCR.

Mitochondrial Dysfunction

A decrease in mitochondrial membrane potential is an early feature of apoptotic cell death and is considered to mark the point of no return. The mitochondrial potential can be measured by a variety of fluorescent probes, which accumulate into the

mitochondrion, as a function of the membrane potential. Collapse of the mitochondrial membrane potential, due to apoptosis, will result in a diminished ability of these fluorochromes to accumulate in the mitochondria. Next, the translocation of several mitochondrial proapoptotic proteins from the intermembrane space into the cytosol can be measured. These proteins include apoptosis inducing factor, cytochrome *c*, and procaspases 2, 3 and 9. Translocation of these proteins can be visualized immunologically, using specific antibodies [34].

.

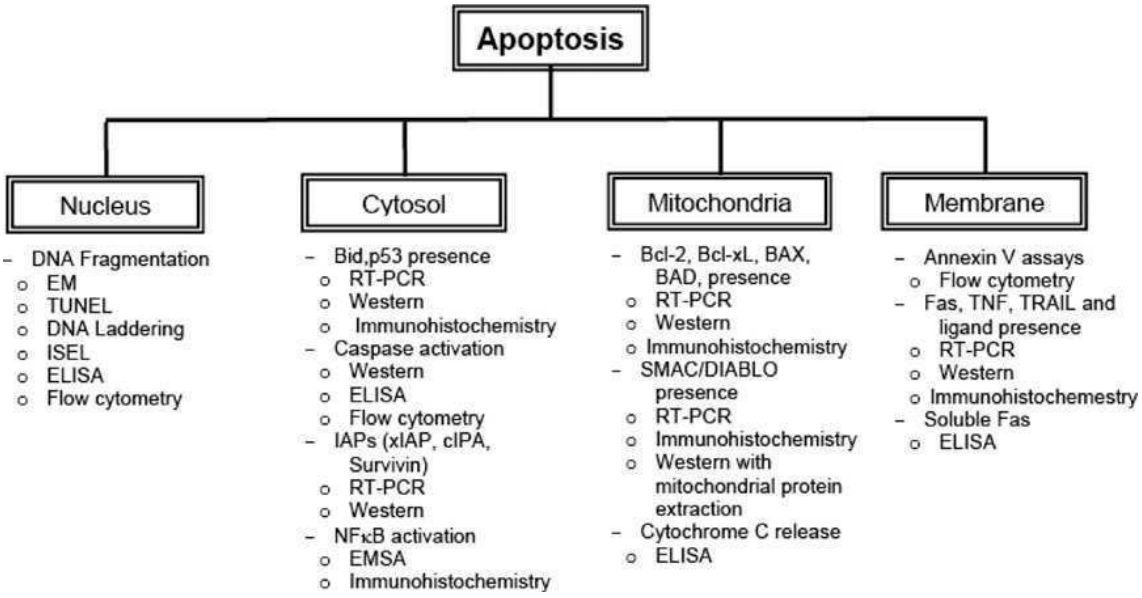

Figure 1.13 Study aspects of apoptosis by various compartments [40].

1.5.1.4 Major Players in Apoptosis

1.5.1.4.1 Caspases

Caspases are specialized proteases that are essential for apoptosis. They are distinct from other proteases because they use a cysteine for catalysis and only cleave after aspartic acid residues. Thus, caspases have an aspartase specificity and must themselves be cleaved twice at aspartic acid residues to generate the active caspase: the first cleavage separates the large and the small subunits whereas the second cleavage liberates the pro-domain [42].

Caspases involved in apoptosis are generally divided into two categories, the initiator caspases, which include caspase-2, -8, -9, and -10, and the executioner caspases, which include caspase-3, -6, and -7. An initiator caspase is characterized by

an extended N-terminal prodomain (≥90 amino acids) important for its function, whereas an executioner caspase contains 20–30 residues in its prodomain sequence.

Once activated, the executioner caspases are responsible for the proteolytic cleavage of a broad spectrum of cellular targets, including structural elements, nuclear proteins, and signaling proteins, leading ultimately to cell death. The known cellular substrates include structural components (such as actin and nuclear lamin), regulatory proteins (such as DNA-dependent protein kinase), inhibitors of deoxyribonuclease (such as DFF45 or ICAD), and other proapoptotic proteins and caspases.

1.5.1.4.2 The Death Receptor Family: Death receptors and ligands

Death receptors belong to the TNF/nerve growth factor superfamily of cell surface receptors, and contain a cytoplasmic protein motif termed the death domain that enables death receptors to engage the cell's apoptotic machinery. Currently, six different death receptors have been identified, including CD95 (APO-1/Fas), TNFRI, DR3 (TRAMP), TRAIL-R1 (DR4), TRAILR2 (DR5) and DR6. Death receptors are activated upon binding to their corresponding ligands or by agonistic antibodies. Death receptor ligands of the TNF superfamily comprise CD95 ligand, TNFa, lymphotoxin-a (this and TNFa bind to TNFRI), TRAIL and TWEAK (a ligand for DR3) [43].

Table 1.1 The correlation between death receptors and their corresponding ligands.

Alternative name of receptors	**Alternative name of ligands**
Fas/APO-1/CD95	FasL/CD95L
TNFR1	TNF-α
DR3/APO-3/SWL-1/TRAMP	APO3L
DR4/TRAIL-R1	APO2L/TRAIL
DR5/TRAIL-R2/KILLER	APO2L/TRAIL

1.5.1.4.3 Adaptor Proteins: FADD, TRADD

Activation of the above death domain-containing receptors by their corresponding ligands can lead to recruitment of intracellular death domain containing adaptors such as Fas associated death domain (FADD) and TNFR associated DD (TRADD). These molecules, in turn cause activation of the caspase cascade and induction of apoptosis [44].

The Fas-associated death domain protein (FADD) is a cytoplasmic adaptor protein and plays an essential role in Fas induced apoptosis. Upon activation of the Fas receptor by FasL, FADD is recruited to the receptor via its carboxy-terminal death domain (DD). The amino-terminal death effector domain (DED) of FADD interacts with a homologous DED within the prodomain of caspase-8 and acts as a platform for caspase-8 recruitment. Upon binding to FADD, caspase-8 is activated by proximity-induced activation and this results in the activation of downstream effector caspases, such as caspase-3, -6 and -7. Once activated, these effector caspases mediate the degradation of various cellular components important for cell structures and integrity, resulting in the characteristic features of apoptosis [45].

1.5.1.4.4 Bcl-2 Family Proteins:

Bcl-2 and its related proteins are important modulators of apoptosis. This family of proteins includes members that inhibit apoptosis (Bcl-2, Bcl-xL, Mcl-1, A1) and promote apoptosis (Bax, Bak, Bad, Bid, Bik, BclxS). Based on sequence alignment, these proteins contain up to four Bcl-2-homology (BH) domains. All of the anti-apoptotic members contain all four domains, while the pro-apoptotic members can be divided into three categories. One group contains BH1, BH2, and BH3 (Bax, Bak), while another group only contains the BH3 domain (Bad, Bid, Bik). Bcl-xS forms its own category, containing both BH3 and BH4 domains.

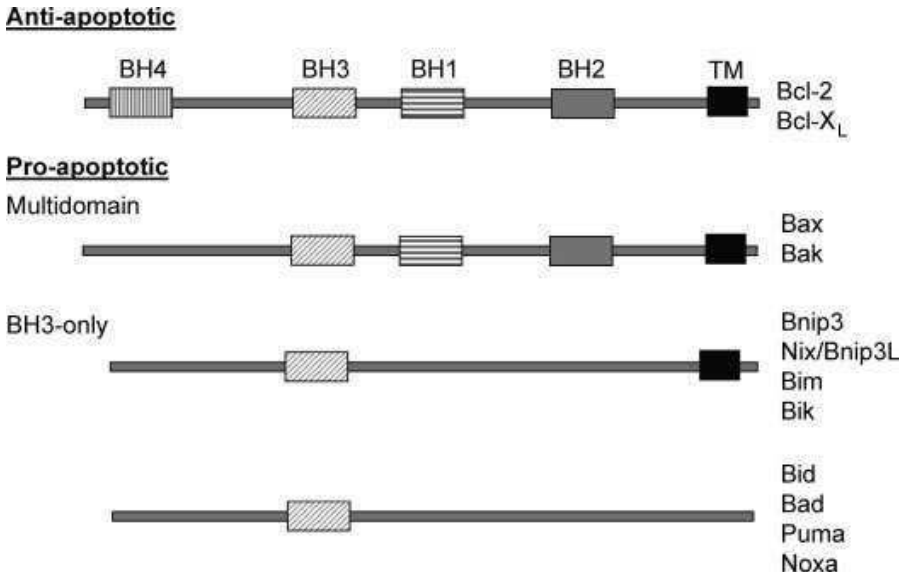

Figure 1.14 Domain structure of Bcl-2 family proteins. Bcl-2 homology (BH) and transmembrane (TM) domains are indicated [46].

It appears that the pro-apoptotic family members BAX and BAK are crucial for inducing permeabilization of the outer mitochondrial membrane (OMM) and the subsequent release of apoptogenic molecules (such as cytochrome *c* and DIABLO (also known as SMAC)), which leads to caspase activation. The anti-apoptotic family members, such as BCL-2 and BCL-XL, inhibit BAX and BAK. Recent evidence indicates that BH3-only proteins de-repress BAX and BAK by direct binding and inhibition of BCL-2 and other anti-apoptotic family members. By contrast, an opposing model postulates direct activation of BAX and BAK by some BH3-only proteins (specifically BIM, tBID and PUMA) [47].

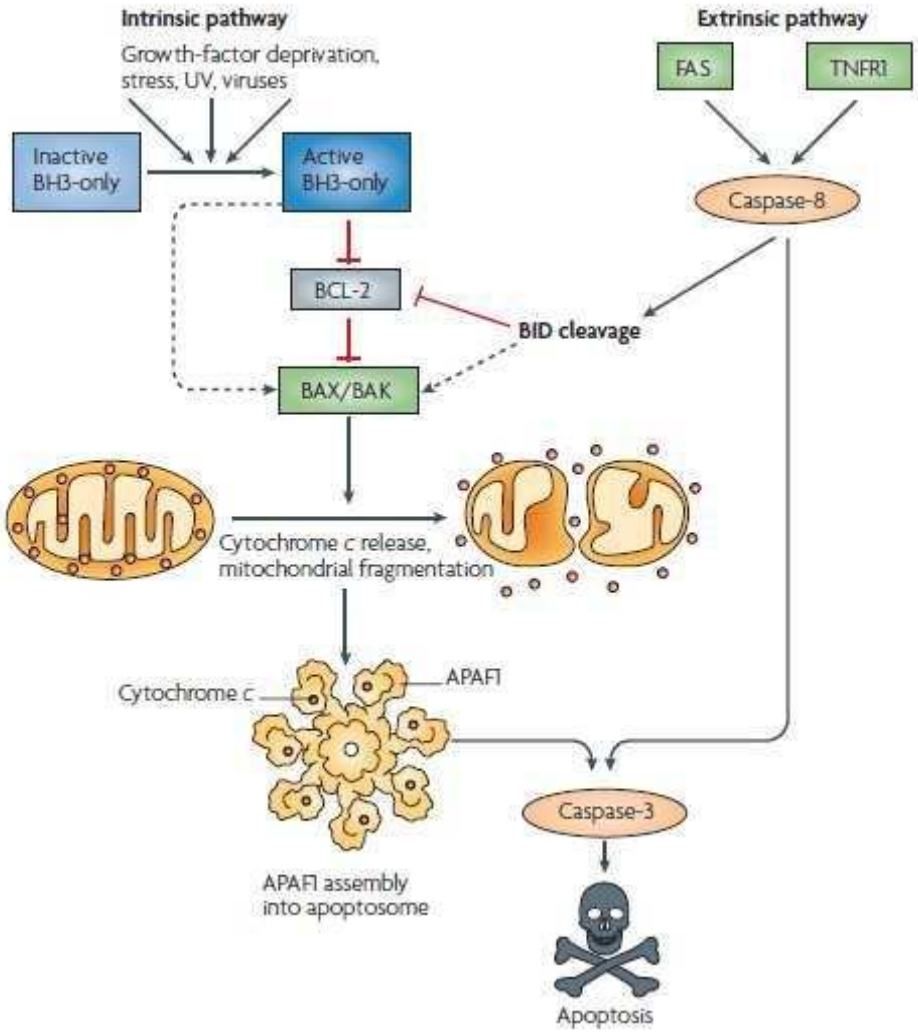

Figure 1.15 Scheme depicting intrinsic and extrinsic pathways of apoptosis [47].

BAX and BAK promote caspase activation by their effects on mitochondria. Either directly or indirectly, these two pro-apoptotic BCL-2 family members induce the release of proteins from the space between the inner and outer mitochondrial membranes. This process of mitochondrial outer membrane permeabilization (MOMP) results in the release of cytochrome *c* and other soluble proteins into the cytosol.

1.5.1.5 Differentiation and Apoptosis

Apoptosis is recognized as a relevant process in neuronal differentiation as well as biological systems. In previous studies it is reported that there is a relation between differentiation and apoptosis. In a study involving *in vitro* neural differentiation of rat marrow stromal stem cells it is indicated that neuronal induction medium (NIM) consisting of BHA, forskolin, DMSO, KCl, valproic acid, B27 supplement contributed 20% of differentiating cells to apoptosis as determined by the TUNEL assay (Jori et al., 2005). Moreover, in another study of Black and Woodbury, analysis of rat marrow stromal cells with TUNEL assay after NIM (consisting of butylated hydroxyanisole, forskolin, N-2 supplement, insulin, DMSO, valproic acid, K252A and KCl) treatment *in vitro* revealed that 1% of total cells were undergoing apoptosis [48].

Yoshiteru Kai *et al.* reported that neural differentiation of mouse embryonic stem cells by the differentiation medium (composed of G-MEM (Gibco) supplemented with 10% KSR (Gibco), 1 mM sodium pyruvate, 0.1 mM nonessential amino acids, 0.1 mM 2-mercaptoethanol and 2 mM L-glutamine) caused 1% of cells to undergo apoptosis [49].

In a study of Milasta et al., treatment of pluripotent PCC7-Mz1 stem cells with 0.1 mM all-trans retinoic acid (RA) causes a cease of proliferation and an initiation of differentiation into neurons, glial cells and fibroblasts. Simultaneously, a fraction of the cell culture (ca. 25%) dies within 24 h by apoptosis. For differentiation, cultures were treated with 0.1 mM (final concentration) all-trans retinoic acid (RA) one day after plating. 24 hours later, the culture medium was replaced byDMEM, supplemented with 12.5% FCS, 0.1 mM RA and 1 mM dibutyryl cAMP [50].

1.5.2 Necrosis

Necrosis is considered to be a toxic process where the cell is a passive victim and follows an energy-independent mode of death. But since necrosis refers to the degradative processes that occur after cell death, it is considered by some to be an inappropriate term to describe a mechanism of cell death. Oncosis is therefore used to describe a process that leads to necrosis with karyolysis and cell swelling whereas apoptosis leads to cell death with cell shrinkage, pyknosis, and karyorrhexis.

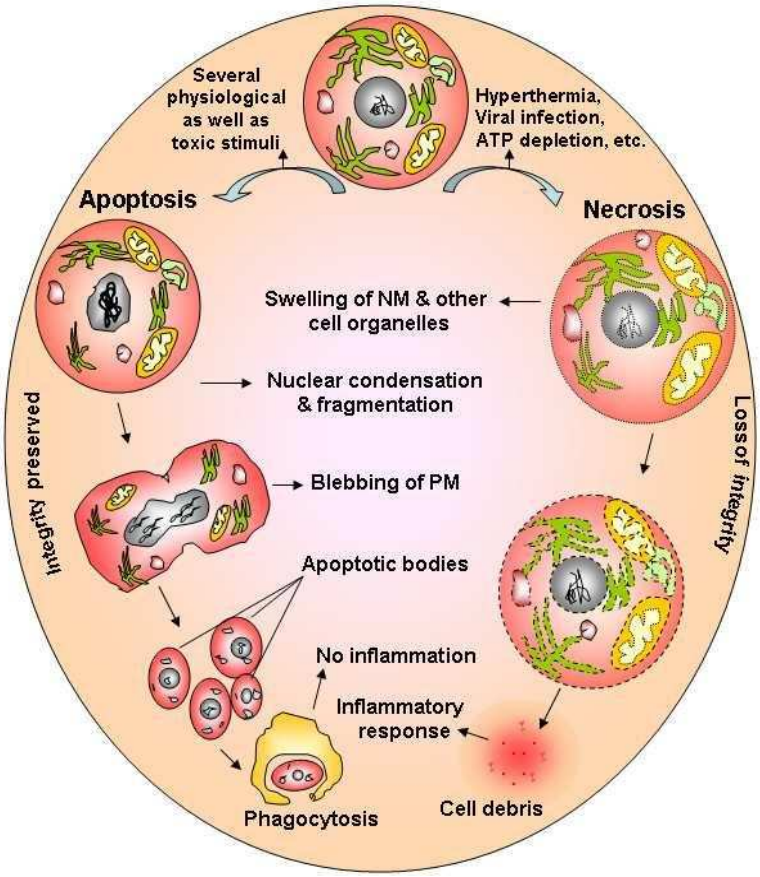

Figure 1.16 Diagrammatic illustration showing the morphological distinctiveness occurring during apoptosis and necrosis [51].

Using conventional histology, it is not always easy to distinguish apoptosis from necrosis, and they can occur simultaneously depending on factors such as the intensity and duration of the stimulus, the extent of ATP depletion and the availability of caspases [52]. Necrosis is an uncontrolled and passive process that usually affects large fields of cells whereas apoptosis is controlled and energy-dependent and can affect individual or clusters of cells. Necrotic cell injury is mediated by two main

mechanisms; interference with the energy supply of the cell and direct damage to cell membranes.

Table 1.2 Comparison of morphological features of apoptosis and necrosis [28].

Apoptosis	Necrosis
Single cells or small clusters of cells	Often contiguous cells
Cell shrinkage and convolution	Cell swelling
Pyknosis and karyorrhexis	Karyolysis, pyknosis, and karyorrhexis
Intact cell membrane	Disrupted cell membrane
Cytoplasm retained in apoptotic bodies	Cytoplasm released
No inflammation	Inflammation usually present

CHAPTER 2

MATERIALS & METHODS

2.1. CELL CULTURE

2.1.1 Mesenchymal stem cell isolation

Bone marrow aspirates were obtained from Şişli Etfal Hospital, Department of Hematology. Ficoll density gradient centrifugation method was used to isolate human mesenchymal stem cells from bone marrow. In this method, bone marrow aspirate (1 ml) was diluted with 9 ml PBS so that the total volume would be 10 ml and 1:10 dilution is performed. Followingly, 5 ml Ficoll was placed in a 15 ml centrifuge tube so that 10 ml diluted bone marrow aspirate was added to the 5 ml ficoll gradient in 2:1 ratio very slowly. Samples were centrifuged at 800 g (2500 rpm) at room temperature (RT) for 25 minutes. After centrifugation, samples were separated into different layers; the bottom, red layer contains red blood cells, the colorless layer on top of that contains Ficoll, white, cloudy layer on top of Ficoll contains mononuclear cells in bone marrow and the top, yellow layer contains sera. Afterwards, the top layer containing sera was discarded and mononuclear cells containing mesenchymal stem cells were transferred into a 15 ml centrifuge tube.

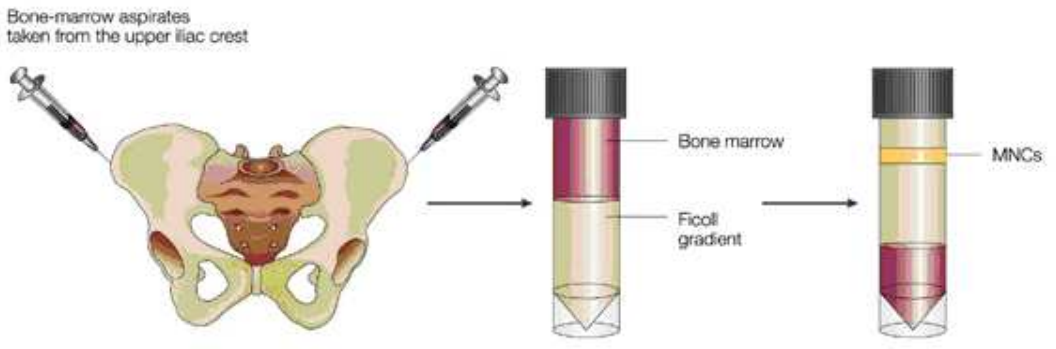

Figure 2.1. Isolation of hMSCs by Ficoll density gradient centrifugation [53].

Next, the volume was completed up to 10 ml with Dulbecco's modified Eagle's medium with low glucose (DMEM-LG, Gibco) and centrifuged at 350g (1500 rpm) for 10 minutes. Supernatant was discarded and cells at the pellet in 0.5 ml medium were resuspended by flicking and pipetting. In order to get rid of the ficoll completely cells were washed with medium again by centrifugation. Again the pellet was resuspended and cells were seeded into a 25 cm^2 tissue culture flask (BD Falcon) in 10 ml DMEM including 20% hMSCs-qualified Fetal Bovine Serum (MSCs-FBS, Gibco) and 0.1 mg/ml Primocin (InvivoGen). Cells were incubated in 5% CO_2 incubator at 37°C and the screw cap of the flask was kept loose in order to allow circulation of carbon dioxide into flask. Until the first subculture, medium was refreshed at 3 days intervals. Non-adherent hematopoietic cells are removed via medium refreshments. When sufficient colonies were formed after 10-14 days, first subculture was carried out.

2.1.2 Subculture and Expansion of hMSCs

As the cells were seeded into the 25 cm^2 flask, the cells became attached to the surface of flask. Thus, adherent primary hMSCs were grown in culture and formed colonies as they were left for proliferation. Nearly 13-14 days later, primary cells were subcultured. Before the subculture, DMEM, trypsin, FBS and PBS were warmed to 37°C in water bath.

Subculture of hMSCs:

1. Medium was discarded from the flask by a sterile pipette.
2. Adherent cells were washed with prewarmed 5 ml PBS (phosphate buffer saline) (Biochrom)
3. Cells were then trypsinized with prewarmed 4 ml of 0.25 % Trypsin/EDTA solution (GIBCO) for 1-2 minutes.
4. As the cells start to detach from the culture surface, tyripsin was neutralized with 1 ml of MSC-FBS.
5. Cell suspension was transferred into a 15 ml centrifuge tube and centrifuged at 350 g (1500 rpm) speed for 10 minutes at room temperature (RT).
6. Supernatant was discarded by leaving ~0.5 ml of the cell suspension at the bottom.

7. Pellet was finger mixed and volume was up to 10 ml with DMEM medium in order to get rid of the remaining tyripsin.
8. Centrifuge was repeated once more. Finally cells were counted by using a hemacytometer (counting chamber) and applied to viability test with Tyrpan Blue (Sigma).
9. 1500 cells/ cm^2 were then seeded into tissue culture flask with DMEM + 15% MSC-FBS and incubated in 37^oC, 5% CO_2 incubator.

Subculture of hMSCs was performed per 6-7 days. Between two passages medium was refreshed one times. Cells were used at 3-5 passages for differentiation and transfection experiments.

2.2 TRANSFECTION

2.2.1 Transfection with Lipofectamine RNAiMAX Reagent

siRNA transfections of hMSCs with Lipofectamine RNAiMAX (Invitrogen) were carried out according to manufacturer's instructions. The day before the transfection cells were seeded into 96-well culture plate with complete medium at 30-50% confluence. ($2x10^3$ hMSCs/well). On the day of transfection, Lipofectamine RNAiMAX was diluted with Opti-MEM in 1:50 ratio. 2 different validated siRNAs (TOP2B_5 and TOP2B_6 from Qiagen) were used for silencing topo IIβ. Sequences of TOP2B_5 and TOP2B_6 are TCGGGCTAGGAAAGAAGTAAA and CAGCCGAAAGACCTAAATACA respectively. Opti-MEM was used to dilute siRNAs in a 1:100 ratio. Diluted siRNA and diluted reagent were mixed in one tube and incubated for 15 min at room temperature to allow the siRNA-Lipofectamine RNAiMAX complexes to form. During this incubation, medium was refreshed with 100 µl, 10% (v/v) FBS containing medium. Followingly, 20 µl of siRNA-Lipofectamine RNAiMAX complexes were added into the wells containing cells and medium, by rocking the plate back and forth. Cells were incubated at 37°C in CO_2 incubator for 24-48 hrs. After 24 hrs incubation, the medium containing complex was removed and replaced by complete medium. Since transfection was performed during neural differentiation, medium was replaced with neurobasal medium containing N3 cytokine combination.

2.3 NEURAL TRANSDIFFERENTIATION OF hMSCs

2.3.1 Neural Differentiation with N3 Cytokine Combinations

The day after transfection, induction experiments were performed. On the day of induction the expansion medium was replaced with 500 µl Neurobasal Medium (GIBCO) containing 2% (v/v) B-27 Supplement (GIBCO), 0.5mg/ml dbcAMP (dibutyryl cyclic AMP, SIGMA), 0.5 mM IBMX (3-isobutyl-1-methylxanthine, SIGMA), 20 ng/ml hEGF (human epidermal growth factor, SIGMA), 40 ng/ml rhFGF (recombinant human fibroblast growth factor, R&D systems), 10 ng/ml FGF-8 (fibroblast growth factor-8, PeproTech), 10 ng/ml rhBDNF (recombinant human brain-derived neurotrophic factor, R&D systems) and 2mM L-Glutamine (GIBCO). This induction medium was refreshed each 48 hours. Morphologies of the cells were observed under invert microscope during 14 days and an apoptotic marker namely caspase 3 expression was monitored at mRNA level with RT-PCR.

2.4 Cytotoxicity (LDH) Assay

The day before the LDH assay (Roche), cells were seeded into 24-well culture plates with complete medium at 30-50% confluency (1x104 hMSCs/well). After siRNA transfection of hMSCs with Lipofectamine RNAiMAX (Invitrogen), cells were incubated at 37°C in a CO_2 incubator for 72 hrs. To determine the LDH activity, 100 µl of cell culture medium was transferred into a 96-well plate at 12, 24, 36, 48, 60 and 72 hrs. Then, 100 µl of the reaction mixture was added to each well and the plate was incubated for 30 min at room temperature, protected from light. The absorbance was then measured in a microplate reader (BioTek) at 490/690 nm.

2.5 Cell Viability and Proliferation Assay

Firstly $2x10^3$ cells/well were seeded into 96-well culture plates with complete medium at 30- 50% confluency. In brief, siRNA transfection was carried out on the next day. After siRNA transfection of hMSCs with Lipofectamine RNAiMAX, cells were incubated at 37°C in a 5% CO_2 incubator for 72 hrs. The WST-1 assay was performed according to the manufacturer's instructions after 24, 48 and 72 hrs of transfection. On the day of WST-1 assay, 10 µl of cell proliferation reagent WST-1 (Roche) was added

to each well and incubated at 37 °C in 5% CO_2 incubator for 4 hrs. The absorbance was measured in a microplate reader (BioTek) at 450/690 nm.

2.6 Real Time Cell Analysis (RTCA)

For time-dependent cell response profiling, 100 µl of media was added to 96 well E-Plates to obtain background readings. After background measurement is performed, the media is discarded from the wells and 100 µl of cell suspension each including 2000 hMSCs was added to each well. 24 hours after seeding the cells, siRNA transfections of hMSCs with Lipofectamine RNAiMAX (Invitrogen) were carried out according to manufacturer's instructions as described above. Followingly, the day after transfection neural induction with N3 cytokine combination is performed. This induction medium was refreshed each 48 hours. The E-Plates containing the cells were placed on the reader in the incubator for continuous recording during 14 days.

2.7 APOPTOSIS ASSAYS

2.7.1 Annexin Assay

Annexin-V-Alexa 568 Staining of Adherent Cells

1. Before staining MSCs are grown on 96 well plates. Transfection and induction experiments are performed and apoptosis is induced in positive control cells by treatment with camptothecin.
2. The medium is removed from the wells 100 µl Annexin-V-Alexa 568 labeling solution is added to each well.
3. 1 µl 50 µM Sytox Green dye is added to each well to differentiate apoptotic cells from necrotic cells.
4. 10–15 min incubation at +15 to +25°C in dark is required.
5. Wells are washed with 200 µl PBS/well, 5 min.
6. Cells are treated with 30 µl 1/15000X DAPI (Sigma) for 10 min at RT for the staining of nuclei.
7. Wells were washed with PBS and dH_2O subsequently
8. The cells were analyzed by flourescence microscopy.

Table 2.1 Essential Solutions used in Annexin-V Staining

Solution	Composition/Preparation
Incubation Buffer	Prepare a solution containing 10mM NaOH, pH 7.4, 140 mM NaCl, 5 mM CaCl2
Annexin-V-Alexa 568 Labeling Solution	Predilute 2 µl Annexin-V-Alexa 568 in 100 µl Incubation buffer for 1 sample.

For positive control samples:

Induction of Apoptosis by Treatment with Camptothecin

Camptothecin, an extract of the Chinese tree *Camptotheca acuminata*, is a potent inhibitor of topoisomerase I, a molecule required for DNA synthesis. Camptothecin has been shown to induce apoptosis in a dose-dependent manner *in vitro*. Camptothecin is routinely used as a general method for inducing apoptosis.

Protocol for Camptothecin-induced Apoptosis:

1. Prepare a 1 mM stock solution of Camptothecin (Sigma) in DMSO.
2. Add 4-6 µM (final concentration) Camptothecin to cell suspension.
3. Perform a time course to obtain optimum results; 2-12 hr incubation at 37°C is suggested.
4. Proceed with assays designed to evaluate induction of apoptosis.

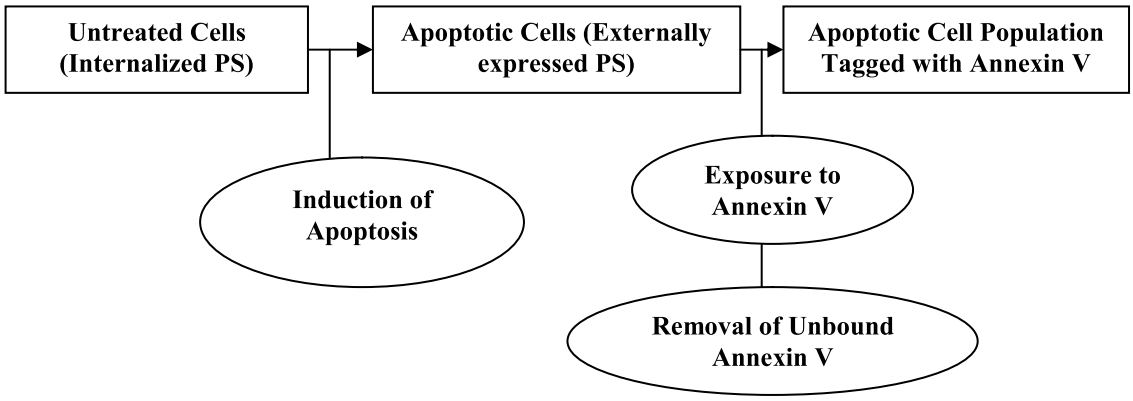

Figure 2.3 Flow chart indicating the method of staining apoptotic cells with Annexin V.

2.7.2 Caspase 3 Detection (RT-PCR)

The apoptotic effect of N3 cytokine combination and siRNA silencing on hMSCs was checked at the mRNA level specifically in caspase 3 expression. RT-PCR technique was used to determine the change in caspase 3 mRNA concentration in various siRNA treated samples and also samples of neurally differentiated hMSCs. From the samples RNA isolation was done by RNeasy kit (Qiagen) according to manufacturer's instructions. Then cDNAs were synthesized by Quantitect reverse transcription kit (Qiagen).These cDNAs were multiplied by PCR with qiagen PCR core kit.

To prepare the genomic DNA elimination reaction master mix, 2 µl of gDNA Wipeout Buffer, the volume of RNA corresponding to 0,5 µg was added in eppendorf tube and then volume was completed to 14 µl with RNase-DNase free water. Then the tube was incubated for 2 min at 42 °C and followingly, tube was placed on ice. The reverse-transcription master mix was obtained by adding 1 µl RT Primer Mix, 4 µl Quantiscript RT Buffer and 1 µl Quantiscript Reverse Transcriptase to the 14 µl RNA mixture to obtain totally 20 µl volume ice. Then, the tube was incubated at 42 °C for 15 min. To inactivate Quantiscript Reverse Transcriptase, tube was incubated for 3 min at 95°C.

In performing the PCR, a 25 µl reaction mixture was prepared by mixing 1 µl of cDNA, 16.8 µl of double distilled water, 0.2 µl of Taq polymerase, 0.5 µl of 10 mM dNTP, 2 µl of 25 mM MgCl2, 1 µl of forward primer, 1 µl of reverse primer and 2.5 µl of 10X Buffer. The PCR conditions were 5 minutes at 94 °C for initial incubation, 30 seconds at 94 °C for denaturation, 45 seconds at 58 °C for annealing of caspase 3 primer, 1 minute at 72 °C for extension and 7 minutes at 72 °C final incubation. The PCR was done for 35 cycles.

Table 2.2. Caspase 3 primer used for quantative RT-PCR

Apoptosis Modulator Gene	**Forward(5'-3')**	**Reverse(5'-3')**	**Annealing Temperature**	**Number of Cycles**	**Size (bp)**
Caspase-3	CTCGGTCTG GTACAGATG TCGATG	GGTTAACC CGGGTAAG AATGTGCA	58°C	35	540

Agarose gel electrophoresis is used to separate PCR products according to their sizes. To visualize the products under UV safe DNA staining solution was used. To prepare % 2 (w/v) agarose gel, 2.6 g of agarose powder (Sigma) and 130 ml of 0.5 X TBE buffer (Fluka) were added to an erlenmeyer flask and boiled in microwave oven. Followingly, the flask was cooled and 27µl safe DNA staining solution was added. Just before it solidifies comb is placed in order to generate 20 wells into 13 x 14x 0.5 horizontal agarose gel platform and then the solution was poured. 100 bp DNA Ladder (Bioron) was used as molecular size marker. To load PCR products on gel, bromophenol blue loading dye was used. Gel was run at 110 V for 45 min.

CHAPTER 3

RESULTS

3.1 SURFACE MARKERS of hMSCs by FACS ANALYSIS

Cell surface markers of bone marrow derived hMSCs at passage 3 were analyzed by fluorescence activated cell sorting (FACS). Flow cytometry results showed that hMSCs at passage 3 expressed CD73 and CD105 whereas they showed a lack of CD34, CD45 and HLA-DR antigens (Figure 3.1).

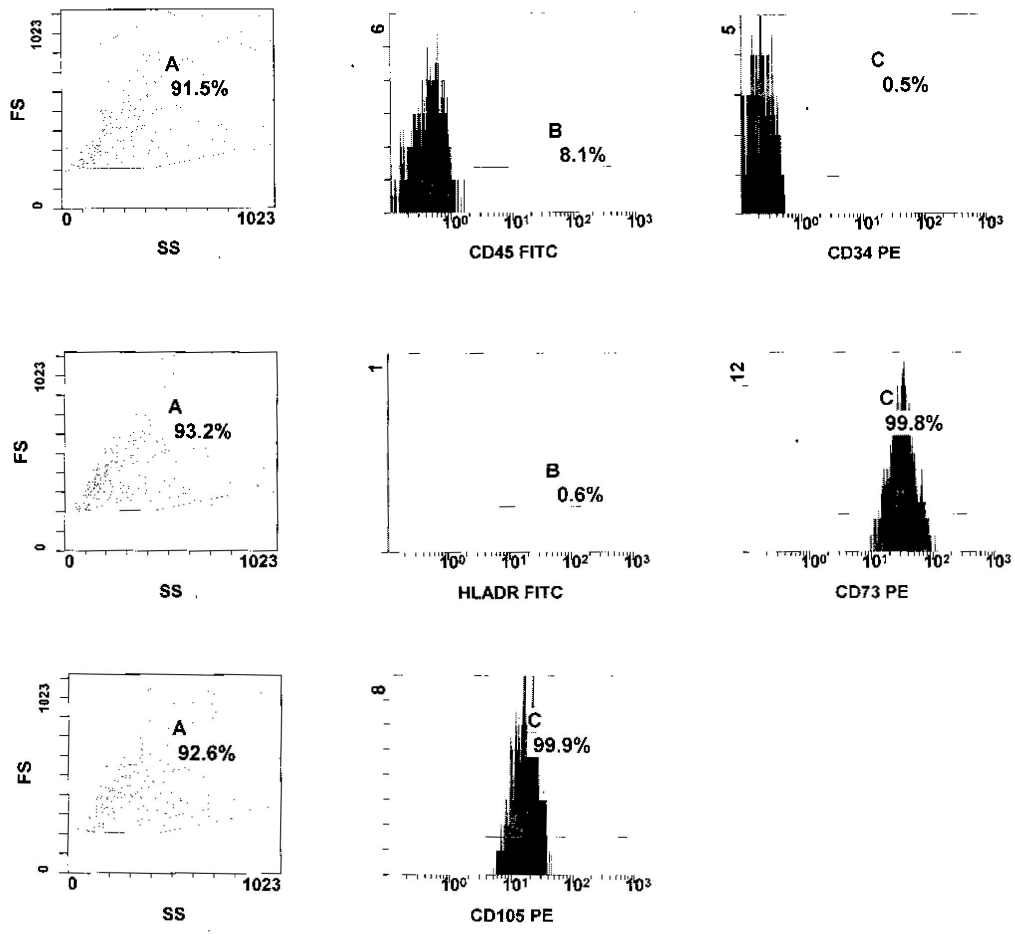

Figure 3.1 Representative flow cytometry analyses of cell surface markers in hBM-MSCs at passage 3.

3.2 hMSCs IN CULTURE

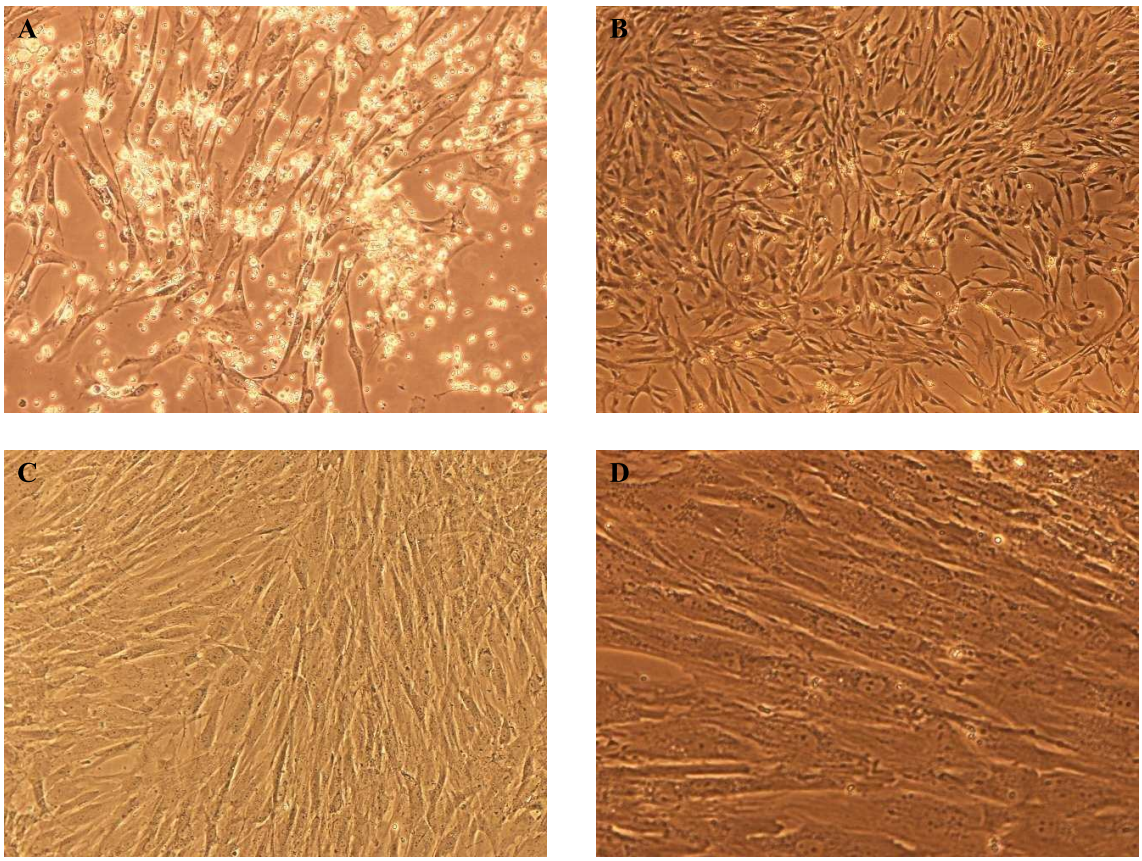

Figure 3.2 Light microscope images of hMSCs in culture. **A.** Primary culture including blood cells in addition to hMSCs (10X), **B.** hMSCs colonies with fibroblastic morphology at passage 3 (4X), **C**. hMSCs at P3 (10X), **D.** hMSCs at P3 (20X).

3.3 NEURAL DIFFERENTIATION WITH N3 CYTOKINE COMBINATION

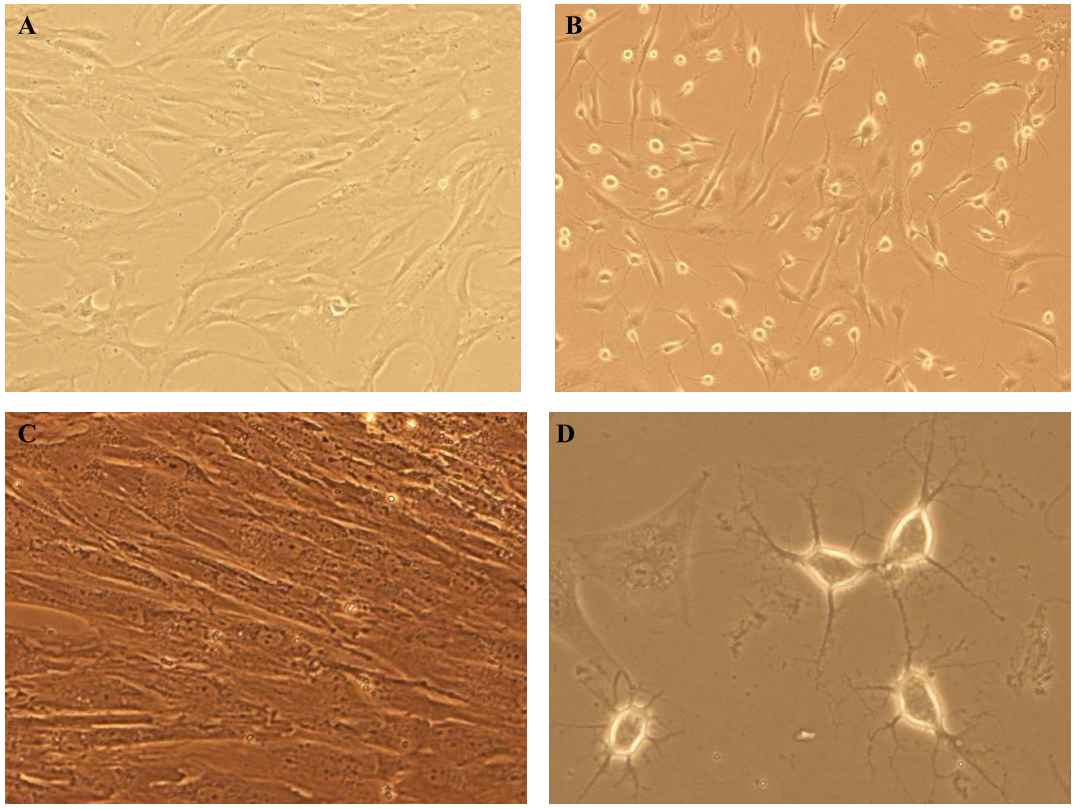

Figure 3.3 Neural differentiation of hMSCs with N3 cytokine combination was observed under light microscope. **A.** Control hMSCs in expansion medium (10X), **B.** Neurally differentiated hMSCs after treatment with N3 cytokine combination (10X), **C.** Control hMSCs in expansion medium (20X), **D.** Neurally differentiated hMSCs (20X).

In the control group, fibroblastic morphology of untreated hMSCs did not change. On the other hand, morphological changes occurred in hMSCs after treatment with N3 cytokine combination; hMSCs differentiated into neural like cells. In addition, 70±10% of hMSCs show neural like morphology in B.

3.3.1 Distinguishing Between N3 Treated and N3+Transfection Treated Groups

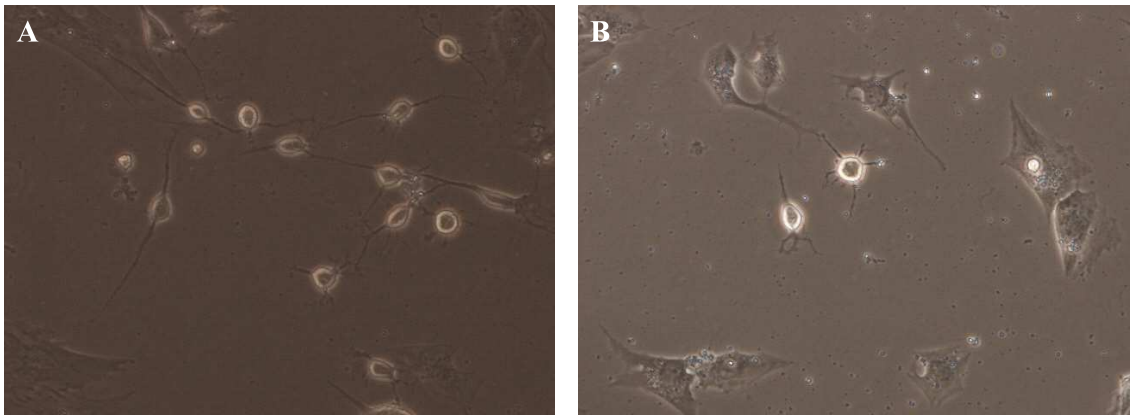

Figure 3.4 The difference in the axon length between N3+Tr and N3 groups.

A. Neurally differentiated hMSCs (15X), **B.** Transfected hMSCs with topo IIβ specific siRNA during neural differentiation (15X).

In the N3+Tr group, length of axon decreases as shown in the above figure. However, in neurally differentiated hMSCs, cells have longer axons. So topo IIβ probably play a role in axon length. When these two groups compared, the length of the axon decreases about 55±5%.

3.4 Cytotoxicity Assay

The cytotoxic effects of Lipofectamine RNAiMAX transfection reagent on 8, 25 and 50 nM topo IIβ specific siRNA transfected hMSCs by Lipofectamine RNAiMAX transfection reagent were measured with LDH cytotoxicity kit. The results are shown in Figure 3.5.

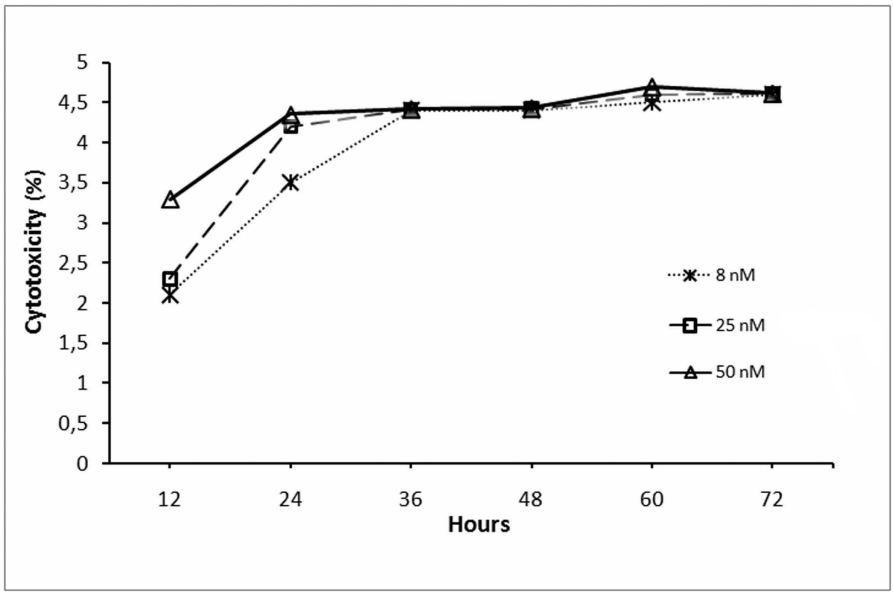

Figure 3.5 Cytotoxicity assays of hMSCs after siRNA transfections with Lipofectamine RNAiMAX. Cytotoxicity of transfected hMSCs increases in the first 24 hours in a dose-dependent manner and then become stabilized in a time-dependent manner.

3.5 Cell Proliferation Assay

The anti-proliferative effects of Lipofectamine RNAiMAX transfection reagent on 8, 25 and 50 nM topo IIβ specific siRNA transfected hMSCs by Lipofectamine RNAiMAX transfection reagent were measured with WST-1 proliferation assay kit. The results are shown in Figure 3.6.

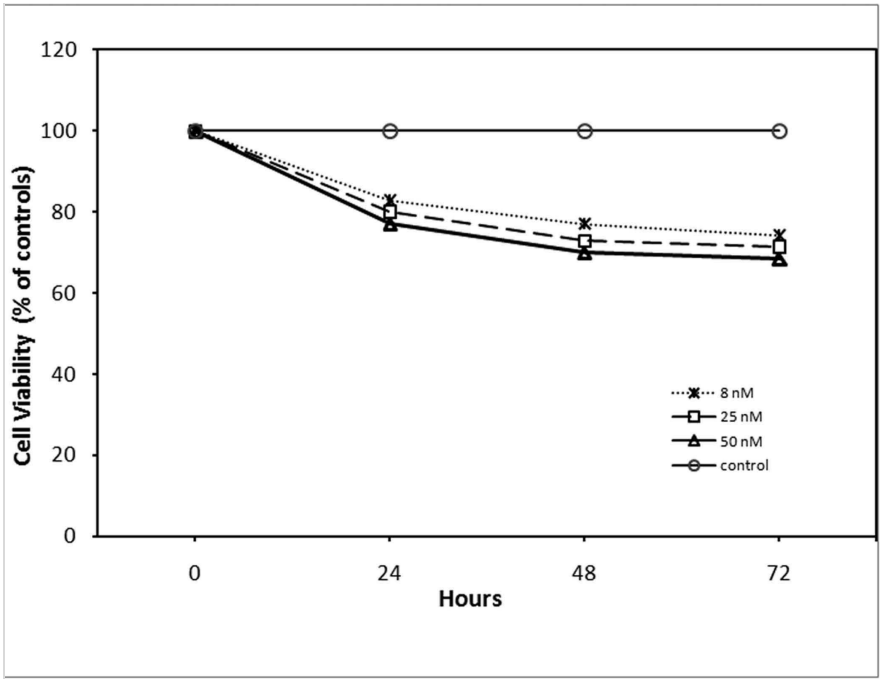

Figure 3.6 Cell viability assay of siRNA transfected hMSCs with Lipofectamine RNAiMAX reagent. Cell viability was affected by Lipofectamine RNAiMAX 20-30% in hMSCs. Transfections were performed twice at 0 and 48 hours.

3.6 Real Time Cell Analysis(RTCA) Results

Beside the specific cytotoxicity and cell proliferation tests we also analyzed N3 cytokine combination and transfection effects on hMSCs with the RTCA (xCelligence) System. The system monitors cellular events in real time by the measurement of electrical impedance across interdigitated micro-electrodes integrated on the bottom of tissue culture 96-well E-plates. The presence of the cells on the top of the electrodes leads to an increase in electrode impedance and is dependent on the cell number and the quality of the cell interaction with the electrodes. Thus, electrode impedance, displayed as cell index (CI) values, can be used to monitor cell viability, proliferation, morphology, and the degree of cell adhesion.

3.6.1 RTCA in Neural Induction by N3 Cytokine Combination

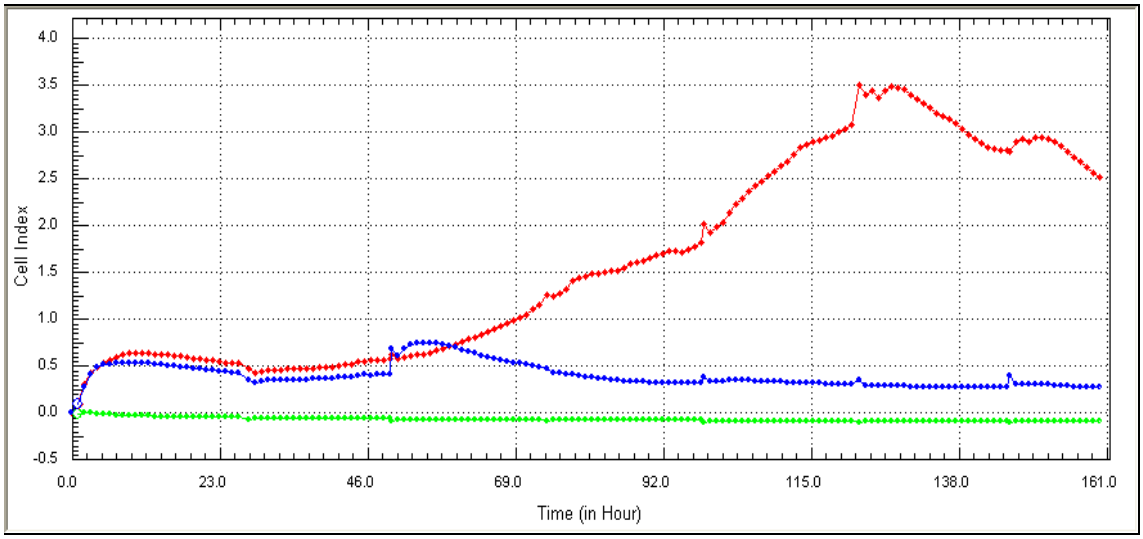

Figure 3.7 Real Time Cell Analysis after neural induction. Blue line, red line and green line representing N3 treated hMSCs, control cells and background readings, respectively.

As shown in Figure 3.7, the index of N3 treated cells decreased compared to control cells. This data indicates that axon formation in N3 treated cells reduced the surface area of the cells and caused changes in impedance signal. Thus, the impedance measurement detected altered morphology and loss of cell adhesion in neurally differentiated hMSCs, therefore, resulting in a lower cell index value.

3.6.2 RTCA in Various Transfection Concentrations

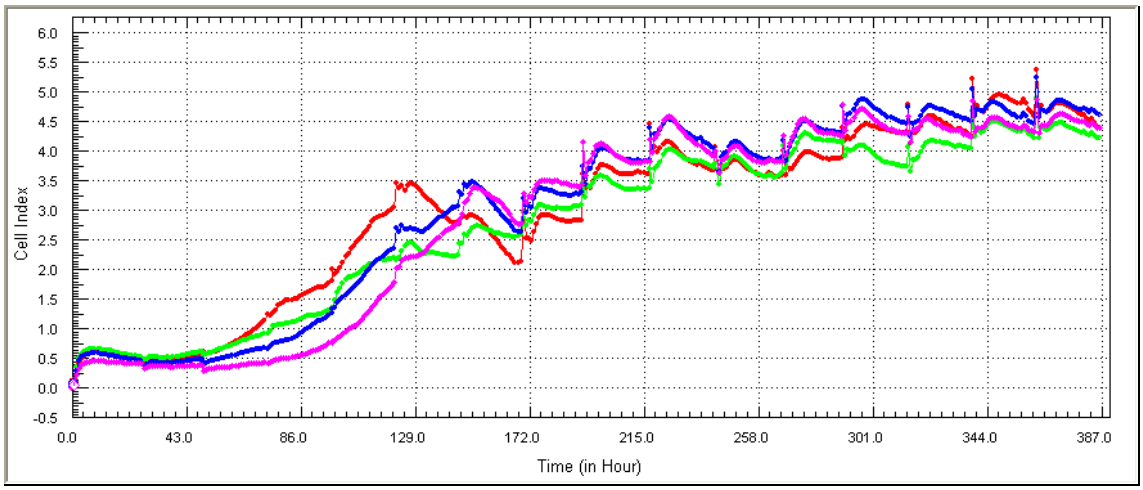

Figure 3.8 Real Time Cell Analysis in 50, 25 and 8 nM siRNA transfected hMSCs. Pink line, blue line, green line and red line representing 50, 25 and 8 nM siRNA transfected hMSCs and control cells, respectively.

Figure 3.8 indicates that at first time there was a difference in cell index between the control group and transfection group however, later cell index value of the transfection group reached control group's standards. Thus, the transfection reagent did not have a toxic effect on hMSCs. Therefore, the impedance measurement in 50, 25 and 8 nM siRNA transfected hMSCs indicates the safety of Lipofectamine RNAiMAX transfection reagent.

3.6.3 RTCA in Various Transfection Concentrations and N3 Treated hMSCs

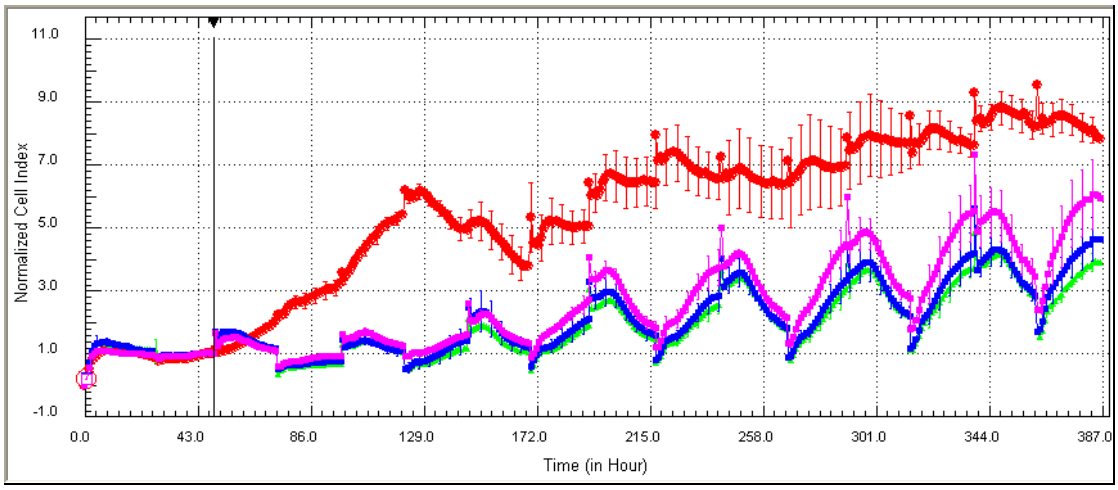

Figure 3.9 Real Time Cell Analysis in 50, 25 and 8 nM siRNA transfected hMSCs during neural induction. Green line, blue line, pink line and red line representing 50 nM, 25 nM, 8 nM siRNA transfected hMSCs together with N3 treatment and control cells, respectively. 24, 72, 120, 168, 216, 264, 312 and 360 hrs showing transfection and 48, 96, 144, 192, 240, 288, 336 and 384 hrs showing induction times.

As shown in the figure, as transfection is performed topo IIβ activity is knocked down and the hMSCs come out of the differentiation pathway, returning to their inherent morphologies thus approaching control group. On the other hand, when induction with N3 cytokine treatment is carried out, cells turned to neuronal morphologies.

3.7 APOPTOSIS ASSAYS

3.7.1 Annexin Assay

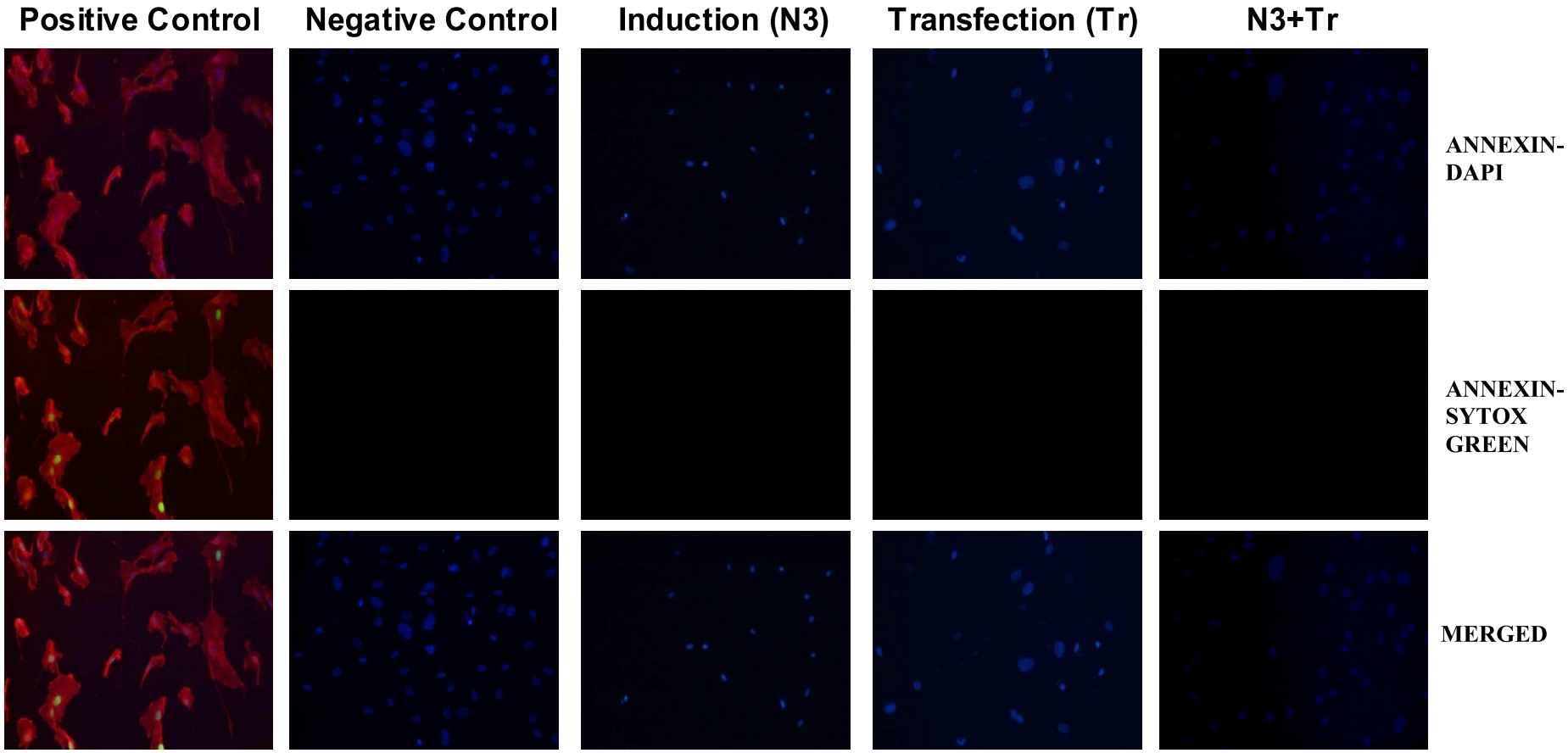

Figure 3.10 Immunofluorescence staining of hMSCs with DAPI, the necrotic marker sytox green and the apoptotic marker annexin under fluorescence microscopy at the end of the 2nd day. All images are at 10X.

The translocation of PS (phosphotidylserine) from the outer to the inner leaflet of the plasma membrane which is an indication of apoptosis was observed with Annexin-V–Alexa 568 assay kit. The results were observed under fluorescence microscopy.

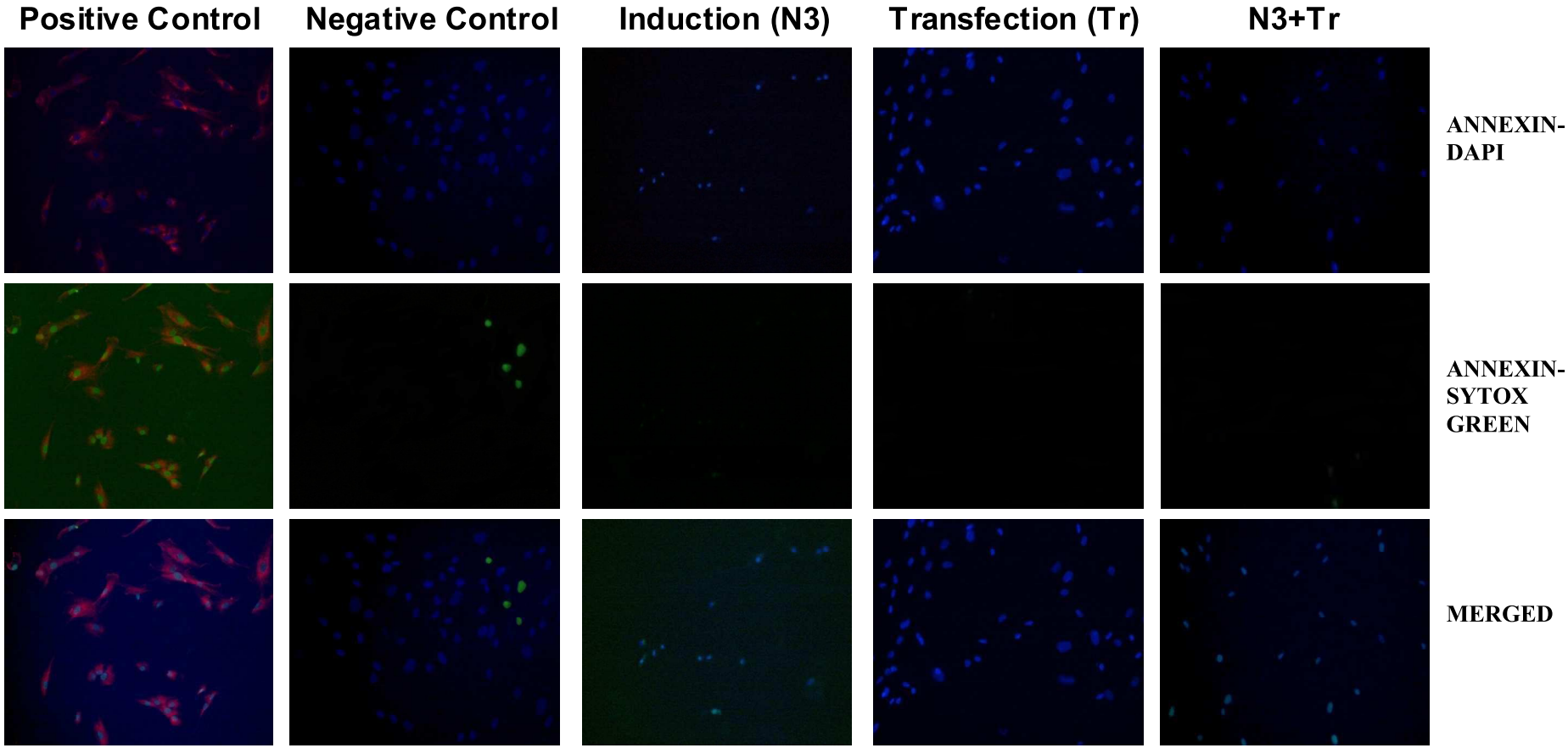

Figure 3.11 Immunofluorescence staining of hMSCs with DAPI, the necrotic marker sytox green and the apoptotic marker annexin under fluorescence microscopy at the end of the 6th day. All images are at 10X.

Camptotechin (CAM) was used to treat the positive control group in the apoptosis assay. Annexin-V Alexa 568 assay kit was applied to Camptotechin treated hMSCs.

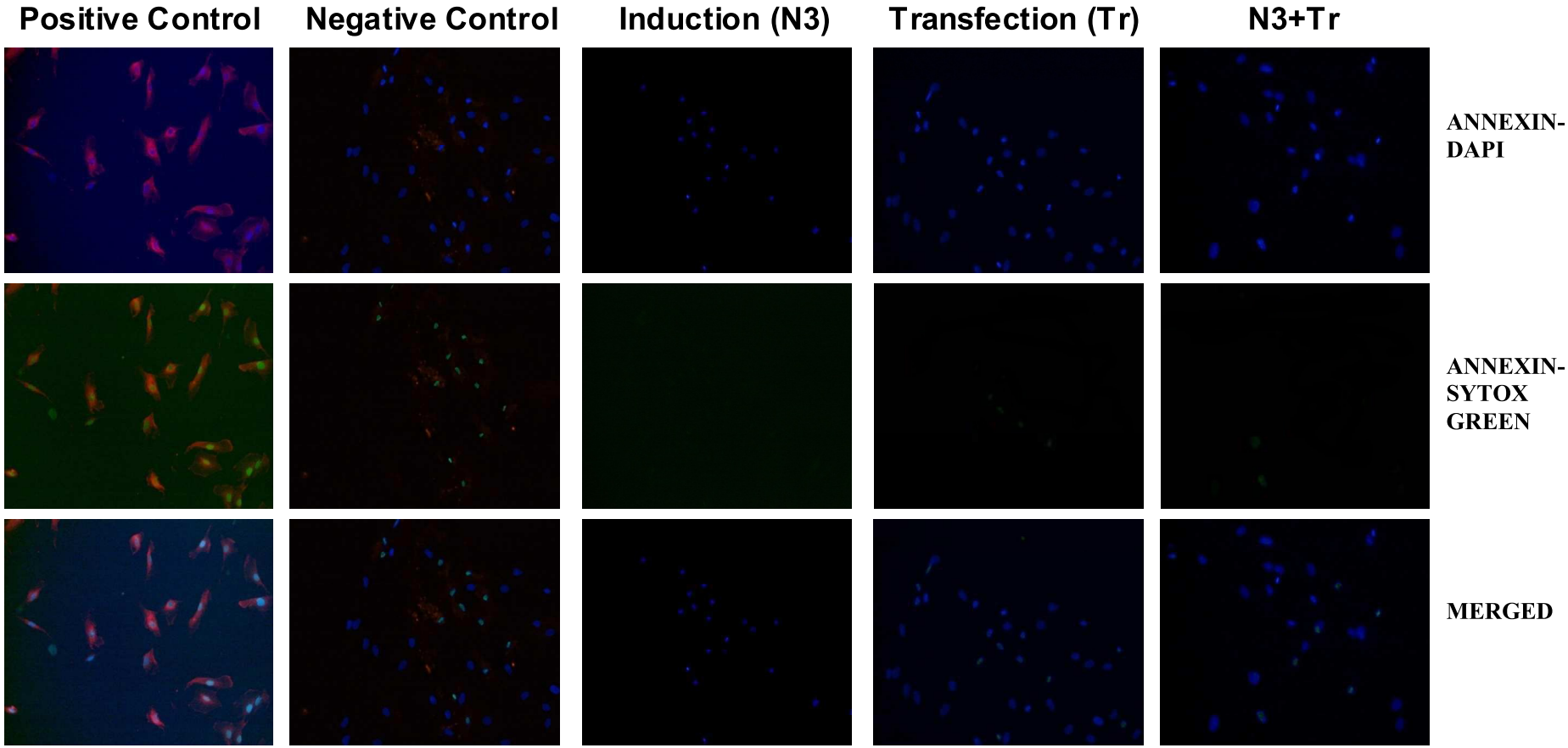

Figure 3.12 Immunofluorescence staining of hMSCs with DAPI, the necrotic marker sytox green and the apoptotic marker annexin under fluorescence microscopy at the end of the 14th day. All images are at 10X.

3.7.1.1 The determination of percentage necrotic and apoptotic cells

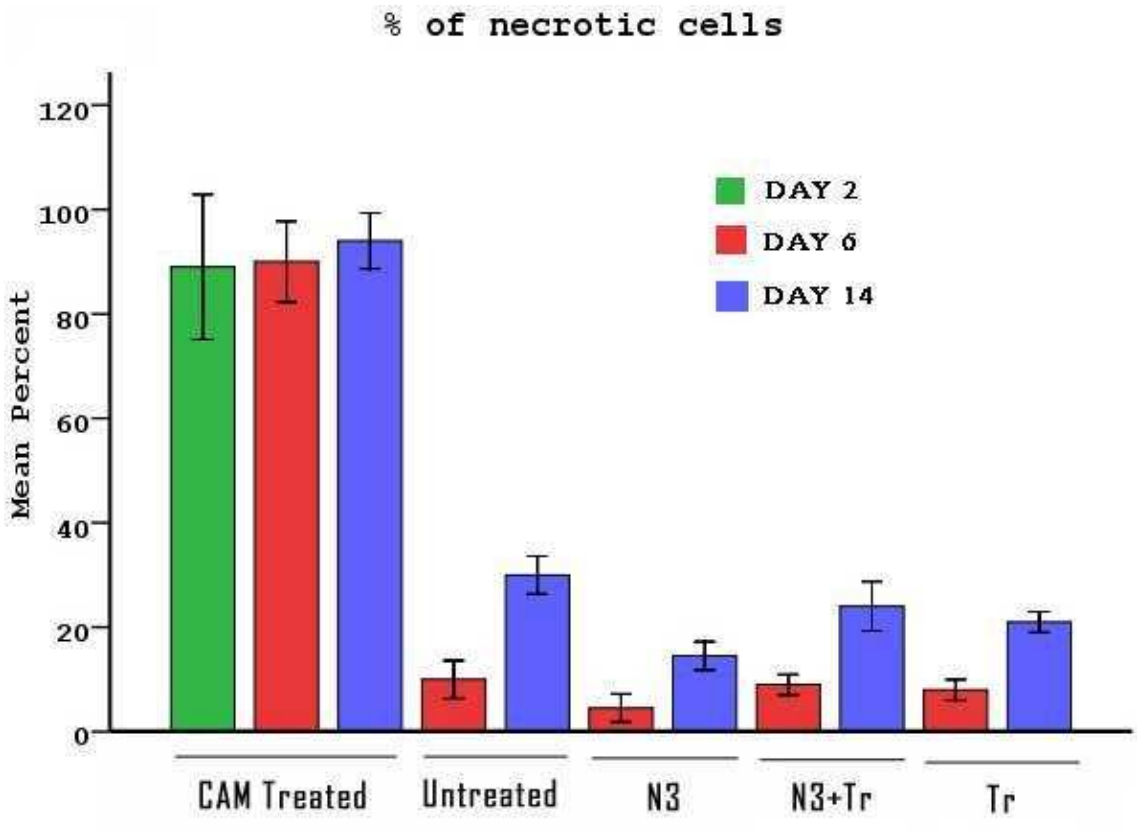

Figure 3.13 The determination of the percentage of necrotic cells in positive control, negative control, induction, transfection and transfection with induction groups at the end of 2^{nd},6^{th} and 14^{th} day. $p<10^{-10}$ (ANOVA; Single Factor)

As shown in Figure 3.13, for the 2^{nd} day 89±11% necrotic cells were examined only for CAM treated positive control. For the 6^{th} day 90±6%, 10±3%, 4.5±2%, 8±1% and 9±1% necrotic cells were reported in CAM treated, untreated negative control, induction, transfection and transfection with induction group, respectively. Next, at the end of the 14^{th} day 94±4%, 20±3%, 10±2%, 15±4% and 13±1% necrotic cells were indicated in CAM treated, untreated negative control, induction, transfection with induction and transfection group, respectively.

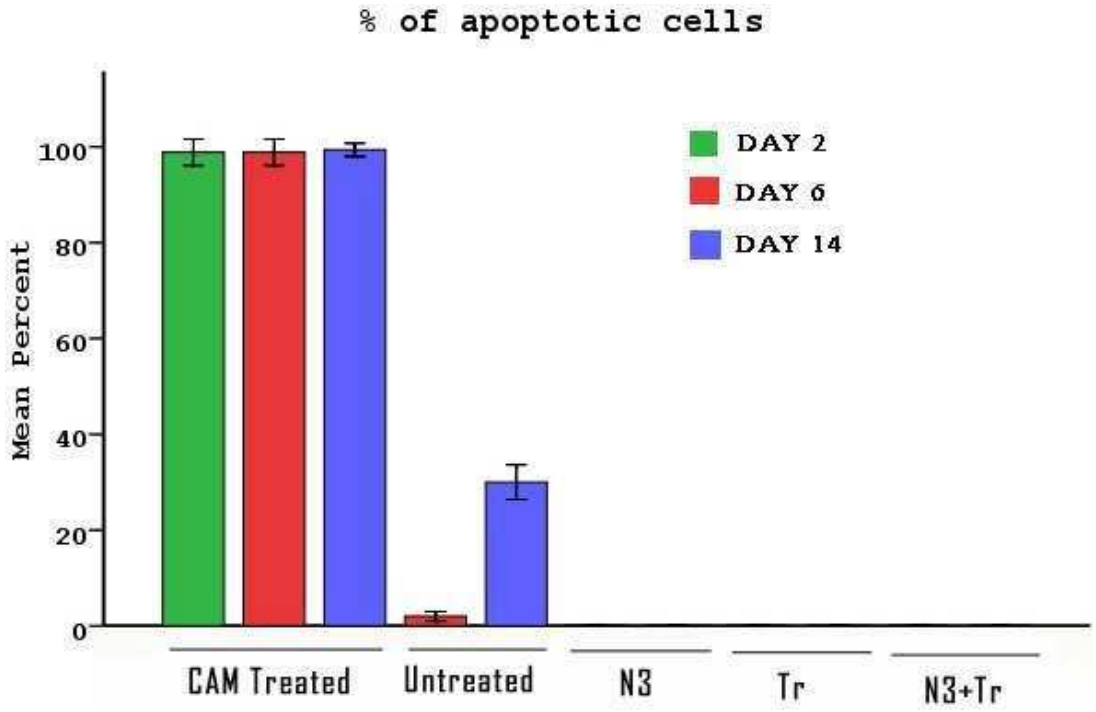

Figure 3.14 The determination of the percentage apoptotic cells in positive control, negative control, induction, transfection and transfection with induction groups at the end of 2^{nd},6^{th} and 14^{th} day. $p<10^{-10}$ (ANOVA; Single Factor).

As shown in Figure 3.14, 99±2%, 99±2% and 99.5±1% apoptotic cells were examined only for CAM treated positive control cells for the 2^{nd} day, 6^{th} day and 14^{th} day, respectively. For the untreated negative control group 1±0.8% and 15±2% apoptotic cells were observed for 6^{th} day and the 14^{th} day, respectively. In the N3 (induction), Tr (transfection) and N3+Tr (transfection during induction) groups apoptotic cells did not occur.

3.7.2 Caspase 3 Detection (RT-PCR Results)

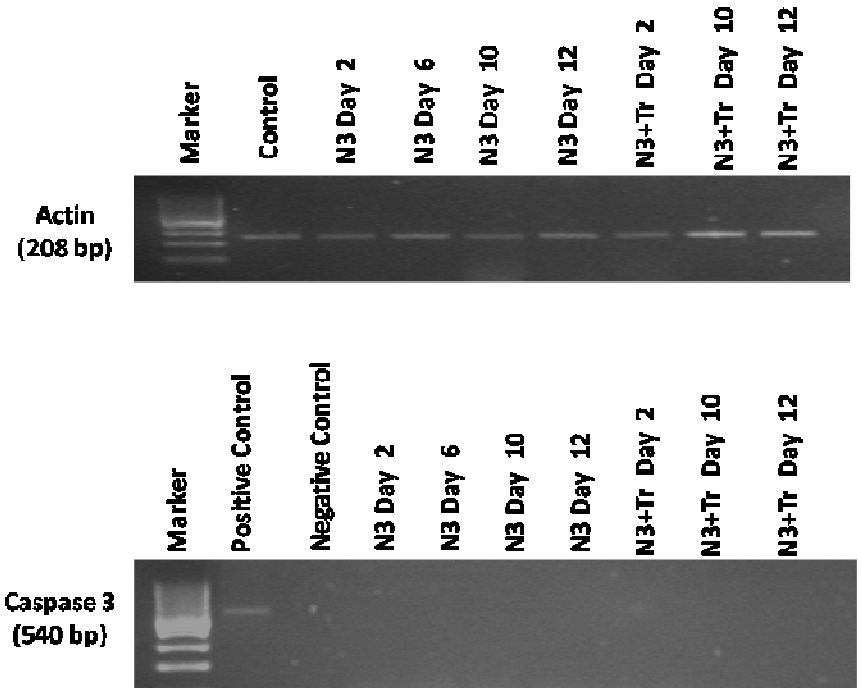

Figure 3.15 RT–PCR results for actin and caspase 3. Neural differentiation was abbreviated N3 and transfection during neural differentiation was abbreviated N3+Tr.

As shown in Figure 3.15, the caspase 3 expression was examined only in the CAM treated positive control group but not in the N3 and N3+Tr groups.

CHAPTER 4

DISCUSSION AND CONCLUSION

Cytotoxicity, cell proliferation and apoptosis are crucial study areas of in vitro cell culture research and are recognized as relevant processes in neuronal differentiation of stem cells. Apoptosis is programmed cell death as signalled by the nuclei in normally functioning human and animal cells when age or state of cell health and condition dictates. Although apoptosis is an important tool for shaping developing organs and for maintaining cellular homeostasis *in vivo,* for neural differentiation *in vitro* it is an undesirable process and it may be caused by neural inducers. Among these inducers chemical agents have the most cytotoxic effect and other inducers like cytokines, growth factors and neurotrophic factors are advantageous in this case. In previous studies the apoptotic effects of various neuronal induction mediums containing chemical agents were indicated. In a study of Black and Woodbury, analysis of rat marrow stromal cells with TUNEL assay after NIM (consisting of butylated hydroxyanisole, forskolin, N-2 supplement, insulin, DMSO, valproic acid, K252A and KCl) treatment *in vitro* revealed that 1% of total cells were undergoing apoptosis [48]. In another study of Jori et al. involving *in vitro* neural differentiation of rat marrow stromal stem cells it is indicated that neuronal induction medium (NIM) consisting of BHA, forskolin, DMSO, KCl, valproic acid, B27 supplement contributed 20% of differentiating cells to apoptosis as determined by the TUNEL assay [54]. Furthermore, Yoshiteru Kai *et al.* reported that neural differentiation of mouse embryonic stem cells by the differentiation medium (composed of G-MEM (Gibco) supplemented with KSR (Gibco), sodium pyruvate, nonessential amino acids, 2-mercaptoethanol and L-glutamine) caused 1% of cells to undergo apoptosis [49].

Regarding cytotoxicity and cell proliferation studies, Warashina et al. indicated that in neural induction of adult hippocampal neural progenitor cells, retinoic acid showed weaker antiproliferation activity and significant cytotoxicity over 2 μm in growth factor (bFGF or LIF/ BMP2)-free basal medium [55]. In another study, Wong et al. examined the effects of two inflammatory cytokines, interferon-γ (IFNγ) and tumour necrosis factor-α (TNFα) on adult neural stem cells. Cytotoxicity assays showed that TNFα but not IFNγ was toxic to the neural stem cells under proliferative conditions. Under differentiating conditions, neither cytokine was toxic; however, IFNγ enhanced neuronal differentiation [56].

In the matter of the current issues, in this study we combined cytotoxicity, cell proliferation and apoptosis experiments and applied them on neural differentiation of hMSCs by N3 cytokine combination. Previously, Long et al. tested this cytokine combination and generated early and mature neural cells [57]. In recent studies it has been suggested that topo IIβ may play a role in neuronal differentiation. Tsutsui et al. showed that topo IIβ is highly expressed in differentiating cerebellar neurons [18]. Thus, in our research we additionally used topo IIβ specific siRNAs during neural differentiation. In other words, we attempted to silence topo IIβ selectively and used Lipofectamine RNAiMAX transfection reagent while introducing topo IIβ specific siRNA to hMSCs. For the aim of understanding the proliferative and cytotoxic effect namely safeness of topo IIβ transfection reagent Lipofectamine RNAiMAX, cytotoxicity and proliferation assays are carried out. Considering this, first of all we tried to prove that Lipofectamine RNAiMAX transfection reagent has low cytotoxicity and high cell viability. Lipofectamine RNAiMAX Transfection Reagent is a cationic lipid-based reagent which is specially produced for the delivery of siRNAs. Zhao et al. indicated that compared to other reagents, Lipofectamine RNAiMAX requires lower concentrations of siRNAs, has minimal cytotoxicity and gives maximal cell viability. Followingly, the use of this reagent in human embryonic stem cells has yielded a 90% transfection efficiency [58].

Secondly, we performed Real Time Cell Analysis (RTCA) in neurally differentiated and siRNA transfected hMSCs in order to monitor the morphology, adhesion, and number of cells in our experiment. Namely, to examine cell viability, number, morphology and degree of cell adhesion in N3 cytokine combination induction

protocol and topo IIβ siRNA transfection protocol Real Time Cell Analysis (RTCA-xCelligence system) was used. In a study of Ehlers et al. involving the effect of okadaic acid on *in vitro* cardiomyocyte differentiation of embryonic stem cells it is indicated that okadaic acid treatment led to rapid morphological changes including cell rounding, the loss of cell-cell contacts and changed electrical impedance as monitored in real time by the xCELLigence system [59].

Lastly, we carried out apoptosis assays involving annexin assay and caspase 3 assay to investigate the apoptotic effect of N3 cytokine combination induction protocol and topo IIβ siRNA transfection protocol.

The integrity of the plasma membrane was evaluated by an LDH assay following 12, 24, 36, 48, 60 and 72 hrs incubating the cells with 8, 25 and 50 nM of topo IIβ specific siRNAs by Lipofectamine RNAiMAX transfection reagent. Relative cytotoxicity of the reagent in transfected hMSCs increases in the first 24 hours in a dose-dependent manner and then become stabilized in a time-dependent manner. The percentage of the damaged cells by the reagent during this time period was approximately in the range of 3.5-4.5%. These results demonstrated that Lipofectamine RNAiMAX did not cause considerable damage to the plasma membrane of hMSCs.

The proliferation assay was performed to elucidate the effect of the same transfection reagent on hMSCs. We established a similar experimental set up as we did for the LDH assay to compare the proliferation rates of the cells treated with 8, 25 and 50 nM of siRNAs after 24, 48 and 72 hrs of transfection. The cell viability of transfected cells decreased about 20% compared to control cells with 8 nM siRNA concentration. The increased concentration of topo IIβ specific siRNAs (25 and 50 nM) did not cause a significant difference in the viability of the transfected cells compared to the lower concentration.

Concerning the cytotoxicity, the transfection of hMSCs with Lipofectamine RNAiMAX caused cytotoxicity in about 3.5- 4.5% of cells. A significant decrease in cell viability was not observed in related with the cytotoxicity. Considering the analysis of these two assays, a negative correlation between the cytotoxicity and cell viability assays was indicated which is a reliable point.

To confirm cytotoxicity and proliferation assays we performed Real Time Cell Analysis (RTCA-xCelligence system). The system monitors cellular events in real time by the measurement of electrical impedance across interdigitated micro-electrodes integrated on the bottom of tissue culture 96-well E-plates. The presence of the cells on the top of the electrodes leads to an increase in electrode impedance and is dependent on the cell number and the quality of the cell interaction with the electrodes. Thus, electrode impedance, displayed as cell index (CI) values, can be used to monitor cell viability, proliferation, morphology, and the degree of cell adhesion. Considering the RTCA results in neural induction, it is shown that the index of N3 treated cells decreased compared to control cells. Abassi et al. reported that the extent of impedance change is proportional to the number of cells inside the well and the inherent morphological and adhesive characteristics of the cells [25]. So, this data indicates that axon formation in N3 treated cells reduced the surface area of the cells and caused changes in impedance signal. Thus, the impedance measurement detected altered morphology and loss of cell adhesion in neurally differentiated hMSCs, therefore, resulting in a lower cell index value.

RTCA in 50, 25 and 8 nM siRNA transfected hMSCs indicates the safety of Lipofectamine RNAiMAX transfection reagent. Although at first time there seems to be a difference in cell index between the control group and transfection group, later cell index value of the transfection group reaches control group's standards.

Concerning RTCA data in transfected hMSCs together with N3 treatment, it is found that as transfection is performed topo IIβ activity is knocked down and the hMSCs come out of the differentiation pathway, returning to their inherent morphologies thus approaching control group. On the other hand, when induction with N3 cytokine treatment is carried out, cells turned to neuronal morphologies. This data indicates that in the absence of topo IIβ, the cells can not continue in the differentiation pathway and the genes related with topo IIβ can not be expressed. Thus, as a preliminary data it is indicated that topo IIβ has a role in neural differentiation.

Apoptosis involves a dynamic interplay of several molecules with up-regulatory and down-regulatory properties like the stimulation of pro-apoptotic molecules or inhibition anti-apoptotic factors. Caspase 3 is an enzyme that plays an important role during apoptosis. In our study we investigated the expression of caspase 3 on hMSCs

after treatment of N3 cytokine combination and siRNA. We found out that caspase 3 is not expressed in our samples showing no apoptosis. Another point to mention is that, although there is no caspase 3 expression in our samples, at the end of the 14th day we reported 20±3%, 10±2%, 13±1% and 15±4% necrotic cells in negative control, induction, transfection and transfection with induction group, respectively. This data, caspase 3 having no relation with necrosis, is consistent with our results since Sinha et al. reported that necrosis does not involve gene expression and it is a passive externally driven process [51].

Necrosis is an unusual and unintended process caused by external cell injury by a number of stimuli. It is characterized by the increase in cell volume followed by enlargement of cell organelles. In this study, for the 6th day we reported 10±3%, 4.5±2%, 8±1% and 9±1% necrotic cells in negative control, induction, transfection and transfection with induction group, respectively. Compared to other groups, negative control group has more necrotic cells probably because of the overconfluency of the untreated cells.

Moreover, in this study, we have obtained neural differentiation of bone marrow isolated hMSCs using N3 cytokine combination. Neural differentiation efficiency in our study is about 70±10%. In addition to that we found that transfected hMSCs had 55±5% shorter axons than the induced hMSCs by N3 cytokine combination. Our data is consistent with the studies of Nur-E Kamal et al. They reported that cortical neurons isolated from top2β knockout mice embryos exhibited shorter neurons indicating the role of topo IIβ in neurite outgrowth [20].

In our study, we did not observe any apoptotic effect on hMSCs. However, we found out that at the end of 6th day little percentage of cells entered necrosis as indicated by the necrotic marker sytox green. Followingly, at the end of 14th day the percentage of necrotic cells increased insignificantly.

All in all, we have shown that Lipofectamine RNAiMAX transfection reagent is safe and useful in terms of cytotoxicity and cell viability and the neural induction protocol by N3 cytokine combination does not lead to apoptosis but causes a negligible level of necrosis.

REFERENCES

[1] S. Bobis, D. Jarocha, and M. Majka, "Mesenchymal stem cells: characteristics and clinical applications," *Folia Histochem Cytobiol,* Vol. 44, No. 4, pp. 215-30, 2006.

[2] S. Gronthos, D. M. Franklin, H. A. Leddy *et al.*, "Surface protein characterization of human adipose tissue-derived stromal cells," *J Cell Physiol,* Vol. 189, No. 1, pp. 54-63, Oct, 2001.

[3] K. Igura, X. Zhang, K. Takahashi *et al.*, "Isolation and characterization of mesenchymal progenitor cells from chorionic villi of human placenta," *Cytotherapy,* Vol. 6, No. 6, pp. 543-53, 2004.

[4] M. S. Tsai, J. L. Lee, Y. J. Chang *et al.*, "Isolation of human multipotent mesenchymal stem cells from second-trimester amniotic fluid using a novel two-stage culture protocol," *Hum Reprod,* Vol. 19, No. 6, pp. 1450-6, Jun, 2004.

[5] Z. J. Liu, Y. Zhuge, and O. C. Velazquez, "Trafficking and differentiation of mesenchymal stem cells," *J Cell Biochem,* Vol. 106, No. 6, pp. 984-91, Apr 15, 2009.

[6] S. M. Devine, and R. Hoffman, "Role of mesenchymal stem cells in hematopoietic stem cell transplantation," *Curr Opin Hematol,* Vol. 7, No. 6, pp. 358-63, Nov, 2000.

[7] N. Boiret, C. Rapatel, R. Veyrat-Masson *et al.*, "Characterization of nonexpanded mesenchymal progenitor cells from normal adult human bone marrow," *Exp Hematol,* Vol. 33, No. 2, pp. 219-25, Feb, 2005.

[8] M. Baddoo, K. Hill, R. Wilkinson *et al.*, "Characterization of mesenchymal stem cells isolated from murine bone marrow by negative selection," *J Cell Biochem,* Vol. 89, No. 6, pp. 1235-49, Aug 15, 2003.

[9] H. K. Vaananen, "Mesenchymal stem cells," *Ann Med,* Vol. 37, No. 7, pp. 469-79, 2005.

[10] S. Ghannam, C. Bouffi, F. Djouad *et al.*, "Immunosuppression by mesenchymal stem cells: mechanisms and clinical applications," *Stem Cell Res Ther,* Vol. 1, No. 1, pp. 2, 2010.

[11] F. Dazzi, R. Ramasamy, S. Glennie *et al.*, "The role of mesenchymal stem cells in haemopoiesis," *Blood Rev,* Vol. 20, No. 3, pp. 161-71, May, 2006.

[12] C. Krabbe, J. Zimmer, and M. Meyer, "Neural transdifferentiation of mesenchymal stem cells--a critical review," *APMIS,* Vol. 113, No. 11-12, pp. 831-44, Nov-Dec, 2005.

[13] D. S. Farbod Rastegar, Jiayi Huang, Wenli Zhang, Bing-Qiang Zhang, Bai-Cheng He, Liang Chen, Guo-Wei Zuo, Qing Luo, Qiong Shi, Eric R Wagner, Enyi Huang, Yanhong Gao, Jian-Li Gao, Stephanie H Kim, Jian-Zhong Zhou, Yang Bi, Yuxi Su, Gaohui Zhu, Jinyong Luo, Xiaoji Luo, Jiaqiang Qin, Russell R Reid, Hue H Luu, Rex C Haydon, Zhong-Liang Deng and Tong-Chuan He., and D. S. Farbod Rastegar, Jiayi Huang, Wenli Zhang, Bing-Qiang Zhang, "Mesenchymal stem cells: Molecular characteristics and clinical applications," *World J Stem Cells,* Vol. 2, No. 4, pp. 67-80, 2010.

[14] F. P. Barry, and J. M. Murphy, "Mesenchymal stem cells: clinical applications and biological characterization," *The International Journal of Biochemistry & Cell Biology,* Vol. 36, No. 4, pp. 568-584, 2004.

[15] K. D. Corbett, and J. M. Berger, "Structure, molecular mechanisms, and evolutionary relationships in DNA topoisomerases," *Annu Rev Biophys Biomol Struct,* Vol. 33, pp. 95-118, 2004.

[16] J. C. Wang, “Cellular roles of DNA topoisomerases: a molecular perspective,” *Nat Rev Mol Cell Biol,* Vol. 3, No. 6, pp. 430-40, Jun, 2002.

[17] B. A. J. Alberts, Julian Lewis, Martin Raff, Keith Roberts, and Peter Walter; Copyright © 1983, 1989, 1994, Bruce Alberts, Dennis Bray, Julian Lewis, Martin Raff, Keith Roberts, and James D. Watson, *Molecular Biology of the Cell*, 4 ed., New York: Garland Science, 2002.

[18] K. Tsutsui, K. Tsutsui, K. Sano *et al.*, “Involvement of DNA Topoisomerase IIβ in Neuronal Differentiation,” *Journal of Biological Chemistry,* Vol. 276, No. 8, pp. 5769-5778, 2001.

[19] X. Yang, W. Li, E. D. Prescott *et al.*, “DNA topoisomerase IIbeta and neural development,” *Science,* Vol. 287, No. 5450, pp. 131-4, Jan 7, 2000.

[20] E. K. A. Nur, S. Meiners, I. Ahmed *et al.*, “Role of DNA topoisomerase IIbeta in neurite outgrowth,” *Brain Res,* Vol. 1154, pp. 50-60, Jun 18, 2007.

[21] S. Rutz, and A. Scheffold, “Towards in vivo application of RNA interference - new toys, old problems,” *Arthritis Res Ther,* Vol. 6, No. 2, pp. 78 - 85, 2004.

[22] GenoTechnology. "CytoScan™ LDH Cytotoxicity Assay," http://www.gbiosciences.com/CytoscanLDHCytotoxicityAssayKit.aspx.

[23] G. D. Roche. "Cell Proliferation Reagent WST-1," http://www.roche-applied-science.com/pack-insert/1644807a.pdf.

[24] K. Solly, X. Wang, X. Xu *et al.*, “Application of real-time cell electronic sensing (RT-CES) technology to cell-based assays,” *Assay Drug Dev Technol,* Vol. 2, No. 4, pp. 363-72, Aug, 2004.

[25] Y. A. Abassi, B. Xi, W. Zhang *et al.*, “Kinetic Cell-Based Morphological Screening: Prediction of Mechanism of Compound Action and Off-Target Effects,” *Chemistry & Biology,* Vol. 16, No. 7, pp. 712-723, 2009.

[26] L. Galluzzi, M. C. Maiuri, I. Vitale *et al.*, "Cell death modalities: classification and pathophysiological implications," *Cell Death Differ,* Vol. 14, No. 7, pp. 1237-43, Jul, 2007.

[27] J. C. Reed, "Drug Insight: cancer therapy strategies based on restoration of endogenous cell death mechanisms," *Nat Clin Prac Oncol,* Vol. 3, No. 7, pp. 388-398, 2006.

[28] S. Elmore, "Apoptosis: a review of programmed cell death," *Toxicol Pathol,* Vol. 35, No. 4, pp. 495-516, 2007.

[29] W. Wood, M. Turmaine, R. Weber *et al.*, "Mesenchymal cells engulf and clear apoptotic footplate cells in macrophageless PU.1 null mouse embryos," *Development,* Vol. 127, No. 24, pp. 5245-5252, December 15, 2000.

[30] I. V. Shemarova, "Signaling mechanisms of apoptosis-like programmed cell death in unicellular eukaryotes," *Comp Biochem Physiol B Biochem Mol Biol,* Vol. 155, No. 4, pp. 341-53, Apr, 2010.

[31] J. F. Kerr, A. H. Wyllie, and A. R. Currie, "Apoptosis: A Basic Biological Phenomenon with Wideranging Implications in Tissue Kinetics," *Br J Cancer,* Vol. 26, No. 4, pp. 239-257, 1972.

[32] A. H. Wyllie, "Glucocorticoid-induced thymocyte apoptosis is associated with endogenous endonuclease activation," *Nature,* Vol. 284, No. 5756, pp. 555-556, 1980.

[33] J. D. Robertson, S. Orrenius, and B. Zhivotovsky, "Review: nuclear events in apoptosis," *J Struct Biol,* Vol. 129, No. 2-3, pp. 346-58, Apr, 2000.

[34] D. Taatjes, B. Sobel, and R. Budd, "Morphological and cytochemical determination of cell death by apoptosis," *Histochemistry and Cell Biology,* Vol. 129, No. 1, pp. 33-43, 2008.

[35] R. M. Locksley, N. Killeen, and M. J. Lenardo, "The TNF and TNF Receptor Superfamilies: Integrating Mammalian Biology," *Cell,* Vol. 104, No. 4, pp. 487-501, 2001.

[36] A. Ashkenazi, and V. M. Dixit, "Death Receptors: Signaling and Modulation," *Science,* Vol. 281, No. 5381, pp. 1305-1308, August 28, 1998.

[37] J. A. Trapani, and M. J. Smyth, "Functional significance of the perforin/granzyme cell death pathway," *Nat Rev Immunol,* Vol. 2, No. 10, pp. 735-47, Oct, 2002.

[38] J. Lieberman, and Z. Fan, "Nuclear war: the granzyme A-bomb," *Curr Opin Immunol,* Vol. 15, No. 5, pp. 553-9, Oct, 2003.

[39] W. L. van Heerde, S. Robert-Offerman, E. Dumont *et al.*, "Markers of apoptosis in cardiovascular tissues: focus on Annexin V," *Cardiovasc Res,* Vol. 45, No. 3, pp. 549-59, Feb, 2000.

[40] S. Huerta, E. J. Goulet, S. Huerta-Yepez *et al.*, "Screening and Detection of Apoptosis," *Journal of Surgical Research,* Vol. 139, No. 1, pp. 143-156, 2007.

[41] N. B. B. G. D. Glick, "Signaling pathways and effector mechanisms pre-programmed cell death," *Bioorganic and Medicinal Chemistry,* Vol. 9, pp. 1371-1384, 2001.

[42] Y. Shi, "Mechanisms of caspase activation and inhibition during apoptosis," *Mol Cell,* Vol. 9, No. 3, pp. 459-70, Mar, 2002.

[43] S. Fulda, and K. M. Debatin, "Signaling through death receptors in cancer therapy," *Curr Opin Pharmacol,* Vol. 4, No. 4, pp. 327-32, Aug, 2004.

[44] P. W. Dempsey, S. E. Doyle, J. Q. He *et al.*, "The signaling adaptors and pathways activated by TNF superfamily," *Cytokine Growth Factor Rev,* Vol. 14, No. 3-4, pp. 193-209, Jun-Aug, 2003.

[45] C. P. Lawrence, and S. C. Chow, "FADD deficiency sensitises Jurkat T cells to TNF-alpha-dependent necrosis during activation-induced cell death," *FEBS Lett,* Vol. 579, No. 28, pp. 6465-72, Nov 21, 2005.

[46] A. B. Gustafsson, and R. A. Gottlieb, "Bcl-2 family members and apoptosis, taken to heart," *Am J Physiol Cell Physiol,* Vol. 292, No. 1, pp. C45-51, Jan, 2007.

[47] R. J. Youle, and A. Strasser, "The BCL-2 protein family: opposing activities that mediate cell death," *Nat Rev Mol Cell Biol,* Vol. 9, No. 1, pp. 47-59, Jan, 2008.

[48] G. Munoz-Elias, D. Woodbury, and I. B. Black, "Marrow stromal cells, mitosis, and neuronal differentiation: stem cell and precursor functions," *Stem Cells,* Vol. 21, No. 4, pp. 437-48, 2003.

[49] Y. Kai, C. C. Wang, S. Kishigami *et al.*, "Enhanced apoptosis during early neuronal differentiation in mouse ES cells with autosomal imbalance," *Cell Res,* Vol. 19, No. 2, pp. 247-58, Feb, 2009.

[50] C. Esdar, S. Milasta, A. Maelicke *et al.*, "Differentiation-associated apoptosis of neural stem cells is effected by Bcl-2 overexpression: impact on cell lineage determination," *Eur J Cell Biol,* Vol. 80, No. 8, pp. 539-53, Aug, 2001.

[51] R. P. R. R. R. P. Sinha, "Apoptosis: Molecular Mechanisms and Pathogenicity," *EXCLI Journal,* Vol. 8, pp. 155-181, 2009.

[52] C. J. Zeiss, "The apoptosis-necrosis continuum: insights from genetically altered mice," *Vet Pathol,* Vol. 40, No. 5, pp. 481-95, Sep, 2003.

[53] K. Pantel, and R. H. Brakenhoff, "Dissecting the metastatic cascade," *Nat Rev Cancer,* Vol. 4, No. 6, pp. 448-56, Jun, 2004.

[54] F. P. Jori, M. A. Napolitano, M. A. Melone *et al.*, "Molecular pathways involved in neural in vitro differentiation of marrow stromal stem cells," *J Cell Biochem,* Vol. 94, No. 4, pp. 645-55, Mar 1, 2005.

[55] M. Warashina, K. H. Min, T. Kuwabara *et al.*, "A Synthetic Small Molecule That Induces Neuronal Differentiation of Adult Hippocampal Neural Progenitor Cells," *Angewandte Chemie International Edition,* Vol. 45, No. 4, pp. 591-593, 2006.

[56] G. Wong, Y. Goldshmit, and A. M. Turnley, "Interferon-[gamma] but not TNF[alpha] promotes neuronal differentiation and neurite outgrowth of murine adult neural stem cells," *Experimental Neurology,* Vol. 187, No. 1, pp. 171-177, 2004.

[57] X. Long, M. Olszewski, W. Huang *et al.*, "Neural cell differentiation in vitro from adult human bone marrow mesenchymal stem cells," *Stem Cells Dev,* Vol. 14, No. 1, pp. 65-9, Feb, 2005.

[58] M. Zhao, H. Yang, X. Jiang *et al.*, "Lipofectamine RNAiMAX: an efficient siRNA transfection reagent in human embryonic stem cells," *Mol Biotechnol,* Vol. 40, No. 1, pp. 19-26, Sep, 2008.

[59] A. Ehlers, S. Stempin, R. Al-Hamwi *et al.*, "Embryotoxic effects of the marine biotoxin okadaic acid on murine embryonic stem cells," *Toxicon,* Vol. 55, No. 4, pp. 855-863, 2010.